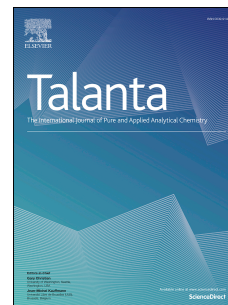


# Journal Pre-proof

Novel microfluidic paper-based analytical devices ( $\mu$ PADs) for the determination of nitrate and nitrite in human saliva

Francisca T.S.M. Ferreira, Raquel B.R. Mesquita, António O.S.S. Rangel



PII: S0039-9140(20)30474-4

DOI: <https://doi.org/10.1016/j.talanta.2020.121183>

Reference: TAL 121183

To appear in: *Talanta*

Received Date: 8 April 2020

Revised Date: 14 May 2020

Accepted Date: 16 May 2020

Please cite this article as: F.T.S.M. Ferreira, R.B.R. Mesquita, A.O.S.S. Rangel, Novel microfluidic paper-based analytical devices ( $\mu$ PADs) for the determination of nitrate and nitrite in human saliva, *Talanta*, <https://doi.org/10.1016/j.talanta.2020.121183>.

This is a PDF file of an article that has undergone enhancements after acceptance, such as the addition of a cover page and metadata, and formatting for readability, but it is not yet the definitive version of record. This version will undergo additional copyediting, typesetting and review before it is published in its final form, but we are providing this version to give early visibility of the article. Please note that, during the production process, errors may be discovered which could affect the content, and all legal disclaimers that apply to the journal pertain.

© 2020 Elsevier B.V. All rights reserved.

**CRedit author statement**

Francisca T. S. M. Ferreira – Methodology; Validation; Formal analysis; Investigation; Writing - Original Draft.

Raquel B. R. Mesquita - Conceptualization; Methodology; Writing - Review & Editing; Supervision; Project administration.

António O. S. S. Rangel – Resources; Writing - Review & Editing; Supervision; Funding acquisition.

## Novel microfluidic paper-based analytical devices ( $\mu$ PADs) for the determination of nitrate and nitrite in human saliva

Francisca T. S. M. Ferreira, Raquel B. R. Mesquita\*, António O. S. S. Rangel

*Universidade Católica Portuguesa, CBQF - Centro de Biotecnologia e Química Fina – Laboratório Associado, Escola Superior de Biotecnologia, Rua Diogo Botelho 1327, 4169-005 Porto, Portugal*

*\*rmesquita@porto.ucp.pt*

### Abstract

In this work, two different microfluidic paper-based analytical devices ( $\mu$ PADs) were developed for the quantification of nitrite and nitrate in human saliva samples, in order to aid in the diagnosis of some diseases and health conditions associated with these ions. The development of these nitrite and nitrate  $\mu$ PADs involved several studies to optimize their design and construction, including an interference assessment and stability studies. These  $\mu$ PADs allowed a nitrite determination in a range of 5 - 250  $\mu$ M with limits of detection and quantification of 0.05  $\mu$ M and 0.17  $\mu$ M, respectively, and a nitrate determination in the range 0.2 – 1.2 mM with limits of detection and quantification of 0.08 mM and 0.27 mM, respectively. As for the stability, both of the  $\mu$ PADs were stable when stored in vacuum at 4°C (the nitrite  $\mu$ PAD for at least 60 days and the nitrate  $\mu$ PAD for at least of 14 days) and, after the sample placement, the nitrite and nitrate  $\mu$ PADs could be scanned within the first 4 and 2 hours, respectively. The nitrite  $\mu$ PAD measurements were compared with the ones obtained from the standard colorimetric method and there were no statistically significant differences between these two methods. To evaluate the accuracy of nitrate  $\mu$ PAD measurements, 4 certified water samples were used and recovery studies using saliva samples were performed.

**KEYWORDS:** *nitrite determination; nitrate reduction; saliva analysis; point-of-care; disposable devices*

## 1. Introduction

According to the World Health Organization, “more people can access essential health services today than ever before, but at least half of the world’s population still go without” basic health care [1]. Even with the advances in technologies, there is still a lack of practical and affordable devices that can perform diagnosis and treatments on location, whether it might be in a medical institution, in the patients’ homes or in the most secluded areas [2,3]. That is why researchers have been working towards the development of new diagnostic and treatment devices and techniques that are “ASSURED”: Affordable, Sensitive, Specific, User-friendly, Rapid and robust, Equipment-free, and Deliverable to end-users [4,5].

In 2007, Martinez A. et al. introduced the concept of microfluidic paper-based analytical device, or  $\mu$ PAD, as a “platform for inexpensive, low-volume, portable bioassays” [6,7]. This type of devices is based on the presence of two different areas: a hydrophilic area provided by the paper where a reaction (usually colorimetric) occurs, and a hydrophobic area that delimits this reaction zone [4,8]. The most common design approach is wax printing, because it is a simple, and relatively fast method compatible with most  $\mu$ PAD applications [4,6]. Nevertheless, this type of printing method requires expensive wax and an extra step of heating in the process. The appeal of the use of paper as a reaction tool is justified not only by the paper’s low cost and high availability, but also by the fact that it is light weighted, available in several thicknesses and porosities, easy to store and transport, and compatible with biological samples (because of its cellulose matrix) [9]. With colorimetric reactions, the most commonly used detection method, the results can be easily interpreted visually or captured with digital cameras, mobile phones or portable scanners [6,8]. Then the color intensities can be obtained from the digital images by using image processing programs and converted to absorbance values [8,10]. A disadvantage of these detection methods is the high variability caused by a non-uniform distribution of the colored product in the paper, but this problem can be reduced by using more replicates and excluding outliers, if necessary [8].

The  $\mu$ PADs popularity is due to their various advantages. They are simple, portable, affordable, rapid, disposable, and, after being assemble, don’t require complex equipment or specialized personnel to do the measurement, which makes them and interesting tool to be used in on-site analysis in locations of difficult access or with very few resources [11]. However, very few of the developed  $\mu$ PADs reported so far, presented any on-field or stability studies [3,8].

Nitrite and nitrate are nitrous acid salts found in the human body due to either an endogenous produce in the body or ingestion through food and water [12,13]. For many years these ions have been associated with cancer, especially nitrite, either from direct ingestion, or the nitrate reduction by bacteria in human saliva. When nitrite reaches the acidic environment of the stomach, and combined with amine or amide, it forms nitrosamines and nitrosamides, which are toxic and carcinogenic, thus contributing mainly to the

development of gastric cancer [13–15]. When absorbed to the bloodstream, nitrite can react with the iron in hemoglobin, irreversibly converting it in methemoglobin and preventing it from carrying oxygen (methemoglobinemia) [13,16–18]. Even though NO<sub>x</sub> compounds have been associated with cancer and other diseases since 1970s, recently a few studies have been reporting newly found benefits of these ions. Salivary nitrates and nitrites may not only be a defense response to oral infectious diseases like periodontal disease [19], but also present a protective effect against dental caries [20].

Several methods have been described for nitrite and nitrate determination, but these methods have some limitations like requiring high volume of reagents and sample, the time of analysis, the use of complex lab equipment, the need of constant power, specialized technicians, the production of toxic waste, among others. These limitations can be emphasized when targeting biological fluids. The most common biological fluid used as samples is blood/serum. However, this type of sample demands an invasive collection procedure with a considerable discomfort to the patient and requiring specialized personnel, very specific storage conditions, together with a risk of contamination and of spreading diseases [21,22]. So, in the last few years there has been an increase in targeting other biological fluids, such as urine and saliva.

The collection of saliva is easier, safer and more economic when compared with blood collection [22–24]. Additionally, it is a painless noninvasive procedure, with a lower risk of contamination or dispersion of contagious diseases [22,23], which does not require specialized medical personnel, and it can be done in secluded areas and more often than the blood collection [21–23]. As a sample, saliva has been known to contain several substances of interest for screening and diagnosis purposes and, although is preferable to be kept on ice, the samples are stable for 24 h at room temperature or for a week at 4°C [11,21,22]. Besides, for some groups of patients, like children, seniors or, for example, patients with blood clotting disorders, it would be easier to collect saliva [22,24]. However, it also has some disadvantages. One of the big issues of using this fluid as a sample is the lack of specific information on biomarker concentrations in saliva, mainly because it is a very recent and new approach [21,23]. Another problem can be the variations in its composition that can occur according to some factors: age, gender, the time of the day of the sample collection and if it was or not stimulated [15,25]. The mean salivary nitrite and nitrate in humans, according to recent studies, was found to be approximately between 1 - 10 mg/L and 10 - 80 mg/L, respectively [12,19,26].

The focus of this work was to develop two new microfluidic paper-based analytical devices (μPADs) for the quantification of nitrite and nitrate anions in human saliva samples, using a new construction approach that has not been reported yet, and based on the Griess reaction for spectrophotometric detection. The idea was for these μPADs to ultimately be capable of being used as a screening option not only in healthcare facilities, but also to aid in the diagnosis of some diseases and health conditions in remote locations.

## 2. Materials and methods

### 2.1. Reagents and solutions

The solutions used in this work were prepared with analytical grade chemicals and Milli-Q water, (resistivity > 18 M $\Omega$ /cm, Millipore, USA).

The standard stock solution of 13 mM sodium nitrite (Merck) was monthly prepared by dissolving approximately 20 mg of the previously dried (overnight 100°C) solid in 25 mL of water. A fivefold dilution of sodium nitrite stock solution (2.5 mM) was weekly made in order to prepare, also weekly, the working standards of nitrite in the range of 5 - 250  $\mu$ M.

The standard stock solution of 12 mM sodium nitrate (Merck) was prepared monthly by dissolving approximately 50 mg of the previously dried (overnight 100°C) in 50 mL of water. The working nitrate standards were prepared daily from the standard stock solution in a range of 0.2 - 1.2 mM.

The Griess reagent was monthly prepared according to Mesquita R. et al. [27] by dissolving approximately 0.4 g of sulfanilamide (Sigma-Aldrich) in 2 mL of 5 M orthophosphoric acid and 0.04 g of N-(1-naphthyl)-ethylenediamine dihydrochloride (N1NED) (Merck) in water. These two homogenized solutions were mixed together, and the volume was completed to 20 mL. This solution was stored in a dark bottle and shielded from the light.

A zinc suspension was prepared for every 4  $\mu$ PADs (maximum), by mixing 1 g of zinc powder (<10  $\mu$ m) (Sigma-Aldrich) in 20 mL of water.

### 2.2 Design of the developed $\mu$ PADs

The assembly of both  $\mu$ PADs consisted in aligning twenty-four sets of filter paper discs units, as hydrophilic area, in a 4 columns and 6 rows distribution, under previously perforated 4 mm holes (for the sample insertion) (L1) made in a 75x110 mm plastic laminating pouch (Q-Connect), as hydrophobic area (Fig. 1).

The nitrite determination  $\mu$ PAD consisted of two layers unit: top layer E1, an empty paper disc (Whatman Grade 1 filter paper 9.5 mm diameter) and G1, the reagent paper disc (Whatman Grade 50 filter paper 9.5 mm diameter) as shown in Fig. 1A. The reagent paper discs were prepared by adding 5  $\mu$ L of the Griess reagent to the discs and then left to dry in the oven for 10 minutes at 50°C.

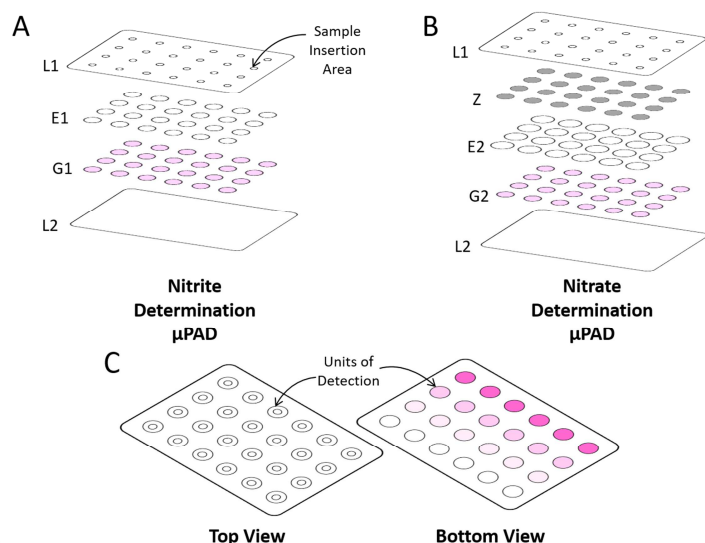


**Fig. 1.** Schematic assembly of the  $\mu$ PAD for the nitrite (A) and nitrate (b) determination and the schematic representation of the device after sample placement; (C); L1, top layer of the laminating pouch; L2, bottom layer of the laminating pouch; E1, empty layer; G1, Griess reagent layer (5  $\mu$ L per disc); Z, zinc embedded layer; E2, empty layer; G2, Griess reagent layer (10  $\mu$ L per disc).

The  $\mu$ PAD for nitrate determination consisted of units of three layers assembled with different sizes and types of paper aligned over each other (Fig. 1B): the top layer Z, zinc suspension paper disc (Whatman Grade 1 filter paper, 9.5 mm diameter); E2, an empty paper disc (Whatman Grade 1 filter paper, 1.27 cm); and G2, the reagent paper disc (Whatman Grade 50 filter paper, 9.5 mm diameter). To prepare the Z layer, the paper discs were embedded in the zinc suspension solution for 30 seconds with manual agitation and then placed in the oven to dry for 30 min at 50°C. Aiming to ensure reproducibility of this procedure, the discs were weighted before and after loading with zinc, in order to maintain an average amount of 2 mg of zinc powder in each disc. The reagent paper discs were prepared by adding 10  $\mu$ L of the Griess reagent to the discs and then placing them in the oven to dry, for 10 minutes at 50°C.

After the alignment of the individual units, the laminating pouches were passed through the laminator (Fellowes L125 - A4), which forces the plastic pouch to melt and seal around the paper filter discs, thus creating a strong physical barrier between the units of detection (Fig. 1C). After the lamination, the  $\mu$ PADs were ready to be use.

The lamination is the most delicate, laborious and susceptible to irreproducibility part of the assembly process, and avoiding the movement of the discs and units is critical. However, that can still happen and, for that reason, it was established to have 6 units for one standard/sample to account for possible outliers due to potential assembly error (and collect the data of 3/4 replicates).

### 2.3. Determination procedure for NO<sub>x</sub> determination

After the  $\mu$ PADs assembly, to perform the measurements, 15  $\mu$ L and 25  $\mu$ L of sample/standard were injected in each sample insertion hole of the  $\mu$ PADs for nitrite and nitrate determination, respectively. When the sample was completely absorbed, the holes were covered with adhesive tape in order to prevent evaporation of the sample and possible contaminations. The sample/standard flows through the layers L1/E1/G1 and L1/Z/E2 (nitrite and nitrate, respectively) until it reacts with the Griess reagent (layer G1/G2), forming a pink color product in which the intensity of the shade of pink is directly proportional to the concentration of nitrite or nitrate in the sample (Fig. 1C).

In order to measure the intensity of the color, the bottom layer of the  $\mu$ PADs were scanned using a standard scanner (Canon LiDE 120) and the images were processed using ImageJ (National Institutes of Health, USA). In this work, the scanning time was considered the period of time between the sample/standard introduction and the scanning of the  $\mu$ PAD.

In the ImageJ, the images were converted into RGB plots. Since the expected colored product of the Griess reaction is pink and the complementary color in which this product absorbs is the green one, the green filter of the RGB plots was used to measure the intensity of pink in the images. For each color disc, an option was made to do the measurements with the circular selection tool with 200x200 pixels, because it allowed better adjustment to the reagent disc area (9.5 mm diameter).

As Birch and Stickle described [10], measured intensities of pink were converted into absorbance values using the formula:  $A = \log_{10}(I_B/I_S)$ , where  $A$  is the absorbance value,  $I_S$  is the average measured intensity (of the pixels) of the standard or sample, and  $I_B$  is the average measured intensity (of the pixels) of the blank. In order to remove outliers, 4 out of the 6 intensity measurements obtained were used in the average calculations.

Regarding the determination of nitrate, the value obtained would correspond in fact to the sum of the content of nitrate plus nitrite (NO<sub>x</sub>), if the reduction process were highly efficient. However, as the nitrite values in saliva are much lower than those of nitrate, no subtraction was needed: Therefore, the sample signal obtained in the  $\mu$ PAD for nitrate determination was directly interpolated in the nitrate calibration curve.



## 2.4. Reference procedures - accuracy assessments

In order to assess the accuracy of  $\mu$ PAD measurements and to validate the developed  $\mu$ PAD for the nitrite determination, a comparison was made between the  $\mu$ PAD measurements and the results obtained by the reference procedure for water analysis [28] since there are no reference methods for saliva analysis. All the solutions were also prepared accordingly.

As no certified saliva samples are available, a certified water sample was used, QC RW1 (VKI reference materials, DANAK) to assess the accuracy of the nitrate  $\mu$ PAD measurements. This certified material consisted of one ampoule with a concentrate for preparation of reference sample by dilution with water. Therefore, 4 rigorous dilutions were prepared, and the final  $\text{NO}_3^-$  concentrations were 0.707 mM (CWS\_1), 0.530 mM (CWS\_2), 0.471 mM (CWS\_3) and 0.354 mM (CWS\_4). Recovery percentages were also calculated for human saliva samples, to which a known concentration of nitrate was added.

## 2.5. Saliva samples collection

The saliva samples used in this work were all collected from healthy volunteers in a range of 20 to 40 years, with their informed consent, by placing a 5x5 cm sterile gauze (Wells) in the mouth for approximately two minutes. The gauze was then placed in a 5 mL sterile syringe and squeezed in order to remove the saliva from the gauze to a 5 mL plastic tube. These samples were diluted to half and were either used immediately (as fresh samples) or stored at  $-20^\circ\text{C}$  for later use (frozen samples).

# 3. Results and discussions

## 3.1. Preliminary studies

As already mentioned, the Griess reaction is perhaps the most commonly known and used reaction for the determination of nitrite. However, there are several ways to prepare the Griess reagent. So, in order to obtain the best sensitivity possible, two compositions of the reagent were tested, both in a batchwise procedure and in filter paper: one reported by Mesquita et al. [27], reagent A (116 mM of sulfanilamide; 500 mM of *ortho*-phosphoric acid; 8 mM of N1NED), and the other by Jayawardane et al. [29], reagent B (50 mM of sulfanilamide; 330 mM of citric acid; 10 mM of N1NED). The chosen reagent was the reagent A, since it presented a higher sensitivity, not only in the batchwise procedure but also on paper (ESM Fig. 1).

As for the nitrate determination, in order to use the same reaction, it was necessary to reduce nitrate to nitrite. Three known reducing agents, namely hydroxylamine, ascorbic acid and tin chloride, were tested alongside with the Griess reagent in a batchwise procedure.

However, there was no formation of the expected pink color, which indicated that neither of the tested reagents were able to extensively reduce nitrate to nitrite. So, it was necessary to consider an alternative; zinc was reported by Jayawardane et al. (2014) [29] to be a powerful reducing agent capable of this conversion. So, a batchwise procedure with the Griess reagent and a Zn powder ( $<10\ \mu\text{m}$ ; Sigma-Aldrich) was prepared and the results confirmed that zinc was an effective reducing agent for nitrate.

### 3.2. Nitrite determination

After testing the reaction in a batchwise procedure and in paper, the next step was to design the  $\mu\text{PAD}$  for nitrite determination. Having set the physical structure of the  $\mu\text{PAD}$  to use a plastic laminating pouch as the hydrophobic area, and filter paper discs for the hydrophilic areas, (24 filter paper discs were used to attain 24 units of detection per  $\mu\text{PAD}$ ) the filter paper layers were studied.

Since there is only one reagent for the nitrite determination, a  $\mu\text{PAD}$  with only one layer of filter paper discs containing the Griess reagent was prepared, corresponding to the G1 in Fig. 1A. However, because the reagent was in direct contact with the air through the sample insertion hole, it oxidized very easily. Moreover, one layer allowed a very limited volume of sample ( $10\ \mu\text{L}$  maximum) and it took a long time to absorb that same volume (30 minutes minimum for  $10\ \mu\text{L}$ ). So, an empty layer (with no reagent) was added on top of the reagent layer (E1 in Fig. 1A) in order to try to protect it from oxidation and also to allow the placement of a higher volume of sample with a smaller absorption time. In this 2-layers  $\mu\text{PAD}$ , the same  $10\ \mu\text{L}$  of sample was completely absorbed in less than 5 minutes.

Several types of filter paper with different treatments and pore diameters available were tested from Whatman® (ESM Table 1). For the reagent layer (G1 in Fig. 1A), the absorbance value obtained for a nitrite standard of  $30\ \mu\text{M}$  was compared for different filter papers (Whatman Grade 1, 42, 50 and 541) using  $10\ \mu\text{L}$  of reagent. The Whatman 50 (W50) paper was the one chosen, as it presented a higher absorbance value.

Then the filter paper of the empty layer (E1 in Fig. 1A) was studied by establishing calibration curves with different filter papers, namely Whatman Grade 1, 5, 42 and 50 together with the W50 paper in the reagent layer (G1 in Fig. 1A). The highest sensitivity, calibration curve slope, was obtained with Whatman Grade 1 (W1) in the empty layer (Fig. 2), together with one of the lowest intercepts (indicating a potentially lower detection limit) so that was the chosen filter paper. This combination of W1 for empty layer and W50 for reagent layer also enabled the  $\mu\text{PAD}$  scanning in least amount of time of all the papers studied (scanning in 20 minutes).

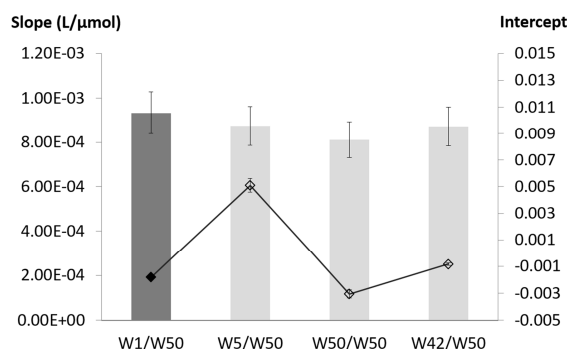


**Fig. 2.** Study of the influence in the calibration curve parameters, slope (grey bars) and intercept (diamonds) of different types of filter paper in the first layer on the nitrite determination  $\mu$ PAD; the chosen combination is represented by the dark grey and black diamond.

After setting the physical parameters, the volume of Griess reagent to place on the reagent layer  $\mu$ PAD was studied. In a preliminary test of the volume capacity of these paper discs, the reagent volumes studied were 5 and 10  $\mu$ L, since lower volumes would not distribute through the entire disc and higher volumes resulted in soaking the disc. Calibration curves were established for both of these volumes and it was possible to observe that there was no significant difference ( $<10\%$ ) between the sensitivities (nor the intercepts). So, to avoid the unnecessary consumption of reagents, a volume of 5  $\mu$ L of Griess reagent per paper disc was chosen for the G1 layer of the nitrite  $\mu$ PAD.

The last parameter tested was the sample volume, and calibration curves were prepared with the standard volumes of 10, 15 and 20  $\mu$ L (Fig. 3A).

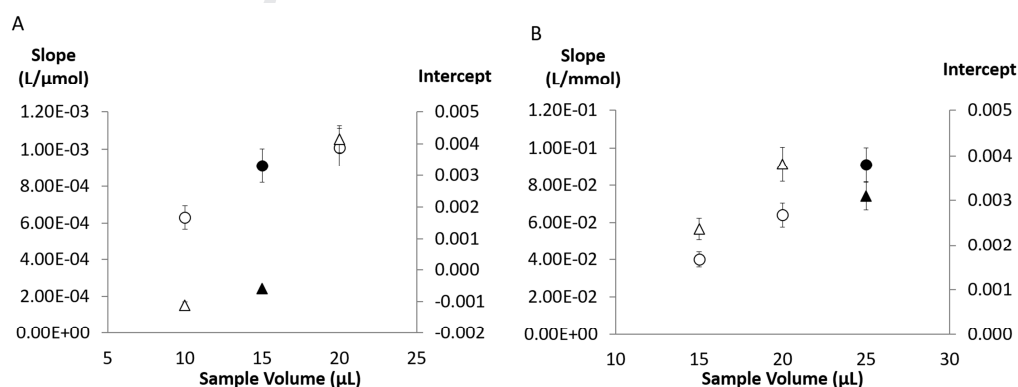


**Fig. 3.** Study of the influence of the reagent volume in the  $\mu$ PADs calibration curve slope ( $\circ$ ) and intercept ( $\Delta$ ) for: A, the nitrite determination and B, the nitrate determination; the points in black represent the chosen values.

When using either 10 or 15  $\mu\text{L}$ , the sample was completely absorbed in approximately 15 minutes. When applying 20  $\mu\text{L}$  of sample, it took about 35 minutes for the  $\mu\text{PAD}$  to completely absorb that sample/standards. Although the highest sensitivity was achieved using the 20  $\mu\text{L}$  of sample, the chosen sample volume was the 15  $\mu\text{L}$ , as a compromise solution between sensitivity and scanning time.

### 3.3. Nitrate Determination

After testing different reducing agents in a batchwise procedure and choosing zinc powder as the reducing agent (preliminary tests), the challenge became placing/immobilizing that powder in the filter paper.

The main concern was the paper low retention capacity and the uneven distribution of the zinc powder. Several procedures were tested, including passing a zinc suspension through the filter paper with a syringe, but the most efficient one consisted in placing the filter paper discs in a zinc suspension (1 g of zinc powder in 20 mL of water), stir the suspension manually and then set the discs to dry (oven at  $50^\circ\text{C}$  for 30 minutes). Therefore, for the nitrate  $\mu\text{PAD}$ , a two-layer assembly was tested, similar to the nitrite  $\mu\text{PAD}$ , but instead of the empty layer (E1 in Fig. 1A) there was the zinc suspension layer (Z layer in Fig. 1B).

However, the direct contact of the Z layer with the Griess reagent layer (G2 layer) caused a visible degradation of the reagent, even before the sample/standard insertion. So, in order to prevent the Griess reagent degradation, an empty layer of filter paper was added between the Z and G2 layers. To ensure that there was no contact, this extra layer (E2 in Fig. 1B) consisted in a W1 filter paper disc with a bigger diameter (1.27 cm) than the other layers (0.95 cm). This approach effectively prevented the reagent degradation and defined the design of the nitrate  $\mu\text{PAD}$  with 3 layers (Fig. 1B).

The assembly of the nitrate  $\mu\text{PAD}$  consisted of detection sets with 3 layers of filter paper: W1, zinc suspension layer (Z in Fig. 1B); W1, empty bigger disc layer (E2 in Fig. 1B); W50, Griess reagent layer (G2 in Fig. 1B). As the targeted concentration range of nitrate was higher than the nitrite concentration range, the influence of the reagent volume was studied again. Calibration curves were set and the same volumes of 5 and 10  $\mu\text{L}$  were tested; 10  $\mu\text{L}$  of Griess reagent produced a 10% increase of the sensitivity, when compared with the 5  $\mu\text{L}$ . Therefore, the chosen volume to be used on the nitrate  $\mu\text{PAD}$  was 10  $\mu\text{L}$  of the Griess reagent.

Because a third layer of paper was introduced in the  $\mu\text{PAD}$ , the  $\mu\text{PAD}$  absorption capability increased significantly. Therefore, it was important to study the influence of the sample volume, and choose the volume that allows a higher sensitivity. So, calibration curves were made, and the sample volumes tested were 15, 20, 25 and 30  $\mu\text{L}$ . With the first three volumes, the sample was completely absorbed into the  $\mu\text{PAD}$  almost immediately, but when 30  $\mu\text{L}$  of sample was used, it took about 35 minutes to observe the sample absorption. Since 35 minutes was considered too much time, the option of 30  $\mu\text{L}$  of sample was

excluded from the study. For the remaining volumes, even though it was possible to scan the  $\mu$ PAD almost immediately after sample introduction, the sensitivity increased for the first 20 minutes. So, to compare the effect of the sample volume, a scanning time of 20 minutes was used (Fig. 3B). Out of the volumes tested, the calibration curve with the highest sensitivity was obtained with 25  $\mu$ L of sample, therefore it was the chosen volume.

In fact, the  $\mu$ PAD for nitrate determination attains the determination of both nitrate and nitrite quantification. This can be explained as any nitrite present goes through the zinc layer (Z in Fig. 1B) to the detection layer (G2 in Fig. 1B) producing the color product. Considering the difference in the expected concentration ranges for nitrite and nitrate, it is not expected to be a significant effect.

However, due to the versatility of these devices, a  $\mu$ PAD for both determinations can be produced (Fig. 4) by assembling two of the four columns identically to the nitrite determination design (one for the introduction of the blank and one for the sample) and the other two columns identically to the nitrate (also one for the introduction of the blank and one for the sample).

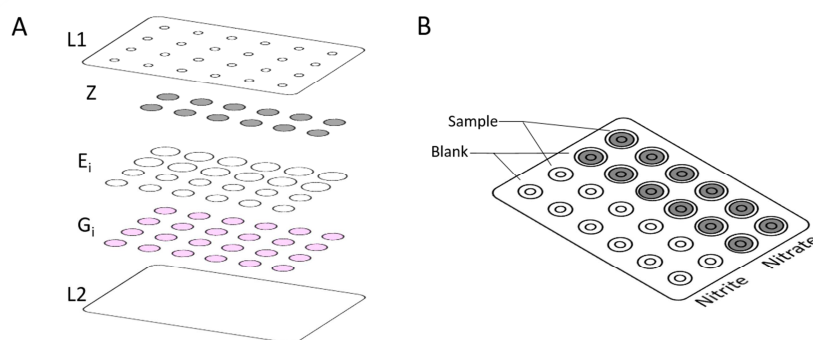


**Fig. 4.** Schematic assembly of the mixed  $\mu$ PAD for determination of both nitrite and nitrate ions; A, alignment; B, finished device.

This mixed design allows the simultaneous determination of nitrite and nitrate ions using one  $\mu$ PAD per sample without compromising the number of replicates (6 detection units per column).

### 3.4. Interferences assessment

To study the interference of the saliva matrix, a set of the developed  $\mu$ PADs were prepared to perform two calibration curves for each determination, nitrite and nitrate using standards in water, and in synthetic saliva.

The synthetic saliva prepared was based on the concentrations reported by Batista et al. [30]: [KCl] = 2237 mg/L; [KH<sub>2</sub>PO<sub>4</sub>] = 544.3 mg/L; [HEPES] = 4766 mg/L; [CaCl<sub>2</sub>·2H<sub>2</sub>O] = 77.69 mg/L; [MgCl] = 19.04 mg/L; [Bovine Serum Albumin] = 2700 mg/L).

For both nitrite and nitrate determination, the use of standards in a synthetic saliva matrix revealed no significant difference on the sensitivity of the calibration curves (< 10%). Therefore, to simplify the process and to reduce the reagents consumption, it was chosen to maintain the use of standards prepared in water, for both the nitrite and nitrate determinations.

### 3.5. Stability Studies

In order to evaluate the robustness of the developed  $\mu$ PADs, stability studies were designed and performed to test the stability of these microfluidic devices not only when stored, before the standard insertion, but also to evaluate the stability of the colored product formed after the standard insertion.

To evaluate the stability of colored product in both of the developed  $\mu$ PADs, a calibration curve for each determination, nitrite and nitrate, was prepared. The  $\mu$ PADs were scanned several times after the standards insertion, up to 4 hours (ESM Fig. 2). The results for the nitrite determination showed there is no significant difference (<10%) between the sensitivity obtained when scanning the  $\mu$ PAD at 20 minutes or 4 hours after the standard insertion. As for the  $\mu$ PAD for nitrate determination initially there was an increase in the sensitivity, up until 1 hour.

This can be explained not only by the existence of an extra layer, but also the existence of a reduction reaction before the color reaction, both of which slow down the formation of the colored product. After reaching a maximum slope (after 1 hour), the sensitivity begins to decrease up to the tested 4 hours. However, the initial increase of sensitivity was not statistically significant when considering a  $\pm 10\%$  range. Whereas, if the  $\mu$ PAD is scanned 3 hours or more after the standard/sample placement, the sensitivity obtained is significantly lower (>18%) than the one obtained up until the 2 hours.

To test the stability of the  $\mu$ PADs before the standard insertion, these devices were prepared and stored, always protected from light, under three different atmospheric conditions (air, nitrogen, and vacuum), both at room temperature (approximately 21°C) and refrigerated (approximately 4°C). The  $\mu$ PADs tested in air atmosphere were stored in a closed clear zip lock bag; the ones in nitrogen atmosphere were stored in a closed clear zip lock bag previously filled with nitrogen gas for approximately 1-2 minutes. The  $\mu$ PADs tested in a vacuum were also stored in a closed clear zip lock bag, in which the air was removed using a vacuum pump. All  $\mu$ PADs were shielded from the light when stored by covering in tin foil. Different periods of time were tested for each of the atmospheric condition.

Every time the  $\mu$ PADs were removed from storage, a calibration curve was set. On the same day, another calibration curve was prepared using the same set of standards, on freshly assembled  $\mu$ PADs. The average sensitivity of these calibration curves was then compared with the sensitivities of the  $\mu$ PADs under the different conditions and a variation under 10% of the average calibration curves was considered non-significant (ESM Fig. 3).

The  $\mu$ PAD for nitrite determination was stable for 3 days for all three storage conditions at room temperature but only when kept in vacuum it was stable for 7 days. When stored in vacuum and refrigerated it was stable for at least 60 days. As for the  $\mu$ PAD for nitrate determination, it was possible to conclude that at the room temperature it was only stable with the storage in vacuum and only for 3 days. Neither the air atmosphere, nor the nitrogen atmosphere were able to appropriately preserve the  $\mu$ PAD for none of the periods of time tested, which is justified by the decrease of the calibration curves sensitivities below the acceptable  $\pm 10\%$  range. When stored in vacuum at fridge temperature, the  $\mu$ PADs for nitrate determination were stable for at least 14 days.

### 3.6. Analytical features of the $\mu$ PAD for NO<sub>x</sub> determination

The main characteristics of the developed  $\mu$ PAD such as dynamic range, average calibration curve, limit of detection (LOD) and quantification (LOQ), relative standard deviation (RSD) and the  $\mu$ PADs optimal scanning time range, are summarized in Table 1.

**Table 1.** Features of the developed  $\mu$ PADs for the determination of nitrite and nitrate; Limit of Detection (LOD); Limit of Quantification (LOQ); Relative Standard Deviation (RSD).

Analyte	Dynamic range	Calibration Curve <sup>a</sup> $A = S \times [\text{NO}_x] + b$	LOD <sup>a</sup> ( $\mu\text{M}$ )	LOQ <sup>a</sup> ( $\mu\text{M}$ )	Repeatability, RSD <sup>b</sup>		Scanning Time
					Intraday	Interday	
Nitrite	5 – 45 $\mu\text{M}$	$y = 1.78 \times 10^{-3} (\pm 5.60 \times 10^{-5}) \times [\text{NO}_2^-] + 1.12 \times 10^{-3} (\pm 3.08 \times 10^{-5})$ $R^2 = 0.997$	0.05	0.17	5%	2%	20 min – 4 h
	45 – 250 $\mu\text{M}$	$y = 1.12 \times 10^{-3} (\pm 3.05 \times 10^{-5}) \times [\text{NO}_2^-] + 3.21 \times 10^{-2} (\pm 2.57 \times 10^{-3})$ $R^2 = 0.996$			2%	3%	
Nitrate	0.27 – 1.2 mM	$y = 7.27 \times 10^{-2} (\pm 8.35 \times 10^{-3}) \times [\text{NO}_3^-] - 2.63 \times 10^{-3} (\pm 1.93 \times 10^{-3})$ $R^2 = 0.988$	80	270	6%	5%	20 min – 2 h

<sup>a</sup> n=6

<sup>b</sup> n=4

Within the nitrite working concentration range 5 – 250  $\mu\text{M}$ , different sensitivities were observed, so this concentration range was divided in two, the range of 5 to 45  $\mu\text{M}$  and the range of 45 to 250  $\mu\text{M}$ .

The limit of detection (LOD) and the limit of quantification (LOQ) were calculated as concentration corresponding to three and ten-times the standard deviation of the intercept ( $n = 6$ ), respectively, according to IUPAC recommendations [31].

The repeatability of the developed  $\mu$ PADs was evaluated calculating the relative standard deviation (RSD) obtained dividing the standard deviation of the calibration slope by the average of that slope. The intraday and interday repeatability were assessed performing 4 calibration curves in the same day and in consecutive days, respectively.

### 3.7. Application of the developed $\mu$ PADs - Accuracy assessment

To assess the accuracy of the developed  $\mu$ PAD for nitrite determination, saliva samples were analyzed using the  $\mu$ PAD ( $[\text{NO}_2^-]_{\mu\text{PAD}}$ ) and the reference method ( $[\text{NO}_2^-]_{\text{Ref.Method.}}$ ) [28]. A linear relationship between the two set of results was established (ESM Fig. 4A):  $[\text{NO}_2^-]_{\mu\text{PAD}} = 1.00 (\pm 0.11) \times [\text{NO}_2^-]_{\text{Ref.Method.}} - 2.74 (\pm 6.82)$ . There was no statistical difference between the two methods, as the slope the intercept were not statistically different from 1 and 0, respectively. The collected samples (#16) were all within the expected range of concentrations (5 – 250  $\mu\text{M}$ ) dues indicating that there would be no cross interference in the nitrate  $\mu$ PAD with dynamic application rate from 0.27 to 1.2 mM.

To evaluate the accuracy of the developed  $\mu$ PAD for nitrate measurements, four dilutions of a certified water sample were used as the certified values were for  $\text{NO}_3^-$ , the same as the  $\mu$ PAD for nitrate determination (Table 2).

**Table 2.** Analysis of certified water samples performed with the nitrate determination  $\mu$ PAD; Standard deviation (SD); Relative deviation (RD)

Sample ID	$[\text{NO}_3^-]_{\text{Found}} \pm \text{SD}$ (mM)	$[\text{NO}_3^-]_{\text{Expected}}$ (mM)	RD%
CWS_1	$0.681 \pm 0.096$	$0.707 \pm 0.014$	-3.6
CWS_2	$0.526 \pm 0.134$	$0.530 \pm 0.011$	-0.7
CWS_3	$0.393 \pm 0.120$	$0.471 \pm 0.010$	-16.7
CWS_4	$0.328 \pm 0.107$	$0.354 \pm 0.007$	-7.2

A linear relationship between the two set of results was established (ESM Fig. 4B):  $[\text{NO}_3^-]_{\mu\text{PAD}} = 1.04 (\pm 0.41) \times [\text{NO}_3^-]_{\text{Certified Value}} - 0.05 (\pm 0.22)$ . Again, there was no statistical difference between the certified value and the  $\mu$ PAD measurement, as the slope and the intercept did not statistically differ from 1 was not and 0, respectively.



To further assess the accuracy of the nitrate measurements, recovery studies were performed by spiking the samples with 4  $\mu\text{L}$  and 8  $\mu\text{L}$  of the nitrate standard stock solution to 1 mL of the saliva sample. The calculation of the recovery percentage was made according to IUPAC [32], amount found minus the initial amount over the amount added (Table 3).

**Table 3.** Recovery studies performed with spiked human saliva samples assessed with the developed  $\mu\text{PAD}$  for nitrate determination; Standard deviation (SD); Relative standard deviation (RSD).

Sample ID	Initial			$[\text{NO}_3^-]_{\text{Added}}$ (mM)	Found			Recovery (%)
	$[\text{NO}_3^-]_{\text{Initial}}$ (mM)	SD	RSD (%)		$[\text{NO}_3^-]_{\text{Found}}$ (mM)	SD	RSD (%)	
SS_1	0.434	0.053	12%	0.216	0.627	0.052	8%	90
SS_2	0.434	0.053	12%	0.431	0.844	0.206	24%	95
SS_3	0.487	0.019	4%	0.216	0.699	0.221	32%	98
SS_4	0.487	0.019	4%	0.431	0.895	0.243	27%	95
SS_5	0.372	0.044	12%	0.216	0.593	0.095	16%	103
SS_6	0.372	0.044	12%	0.431	0.822	0.102	12%	104
SS_7	0.509	0.059	12%	0.216	0.713	0.108	15%	95
SS_8	0.609	0.081	13%	0.431	1.068	0.166	16%	106
SS_9	0.384	0.101	26%	0.216	0.612	0.082	13%	106
SS_10	0.384	0.101	26%	0.431	0.791	0.081	10%	94
SS_11	0.491	0.086	18%	0.216	0.701	0.205	29%	97
SS_12	0.491	0.086	18%	0.431	0.932	0.094	10%	102
SS_13	0.621	0.054	9%	0.216	0.825	0.157	19%	94
SS_14	0.275	0.053	19%	0.216	0.486	0.106	22%	98
SS_15	0.275	0.053	19%	0.431	0.694	0.080	12%	97

The average of the calculated recoveries was 98% with a standard deviation of 5%. A statistical test (t-test) was used to evaluate if the mean recovery value did significantly differ from 100%. For a 95% significance level the calculated t-value was 1.32 with a correspondent critical value of 2.51. The statistical results indicate the absence of multiplicative matrix interferences proving that the developed  $\mu\text{PAD}$  was applicable to saliva samples.

#### 4. Conclusions

In this work, two new microfluidic paper-based analytical devices ( $\mu\text{PADs}$ ) for the nitrite and nitrate quantification in human saliva samples were devised. Additionally, considering their versatile architecture, both determinations can be combined in a single bi-parametric device.

The developed  $\mu$ PADs have shown to be sensitive, portable devices that provide rapid on-hand measurements and were efficient for determinations in human saliva samples, without requiring pre-treatments.

The main application envisioned for these devices was to facilitate health diagnosis, not only in healthcare facilities, but also in remote areas. They are affordable, having a cost (in terms of consumables) of 0.15€ and 0.20€ per nitrite and nitrate  $\mu$ PAD, respectively, and also disposable by incineration, which besides being environmental-friendly, is also an advantage when handling biological samples.

Furthermore, unlike recently reported devices (Table 4) such as Chiang C. et al. (2019), Vidal E. et al. (2018) and Liu Y. et al. (2018) [33–35], this novel construction and assembly technique is very simple and user-friendly, since it doesn't require specialized technicians or complex equipment, like wax printers. This type of printers, commonly used in  $\mu$ PADs preparation, is associated to a substantial investment, costly consumables and not environmental friendly.

**Table 4.** Comparison of some features of this work with previous ones.

Analyte	Concentration range ( $\mu$ M)	LOD ( $\mu$ M)	LOQ ( $\mu$ M)	Sample matrix	Observations	Reference
$\text{NO}_2^-$	5 – 250	0.05	0.17	Saliva	Both determinations can be combined in a single device with a biparametric determination	This work
$\text{NO}_3^-$	200 - 1200	80	270			
$\text{NO}_2^-$	3.9 – 1000	14.8	NR	Water	Wax printed $\mu$ PAD	Chiang [33]
$\text{NO}_2^-$	0.88 – 11.8	0.86	NR	Saliva	Sample Pretreated; Electrokinetic stacking combined with colorimetric reaction	Zhang [36]
$\text{NO}_2^-$	20 – 160	7.8	NR	Saliva	$\mu$ PAD fabrication by corona generator	Jiang [37]
$\text{NO}_2^-$	0.01 – 5.0	$6.2 \times 10^{-5}$	NR	Water	Wax printed $\mu$ PAD; Electrochemical detection	Liu [35]
$\text{NO}_2^-$	1 – 215	0.6	2.8	Water	Wax printed $\mu$ PAD	Vidal [34]
$\text{NO}_2^-$	5 – 500	1.3	2.2	Water	$\mu$ PAD fabrication by a craft-cutting technique	Ortiz-Gomez [38]
$\text{NO}_2^-$	156 – 1250	NR	NR	Water	$\mu$ PAD fabrication by patterning of filter paper using a permanent marker pen.	Wang [39]
$\text{NO}_2^-$	0 – 100	5.6	NR	Saliva	With sample preconcentration	Cardoso [40]
$\text{NO}_2^-$	10 – 150	1	7.8	Water	Inkjet printed $\mu$ PAD; Independent devices for each analyte determination	Jayawardane [29]
$\text{NO}_3^-$	50 – 1000	19	48			

NR, Not Reported.

The improvement in the detection limit can be explained by the  $\mu$ PAD architecture. Most of previously reported  $\mu$ PADs are based either on a one-layer construction, or on folding the paper to create multiple layers. In the first option, the sensitivity can be impaired by the colour dispersion associated with the hori-

zontal flow. In the second option, the 3D  $\mu$ PADs assembled by folding, although it benefits from the vertical flow, the folding of the paper can create air pockets between the layers which compromise the efficiency of the vertical flow between the layers. The novel architecture of developed  $\mu$ PAD uses the advantages of the vertical flow and provides a very low probability of the formation of air pockets that could impair the flow through the layers.

As future work, it would be interesting to perform field studies to further access the impact of conditions different from the ones that exist in the laboratory. Ultimately, the  $\mu$ PADs should be used for analysis in saliva samples of patients with NO<sub>x</sub>-related diseases.

### Acknowledgment

This work was supported by National Funds from FCT - Fundação para a Ciência e a Tecnologia through project UID/Multi/50016/2019.

### Appendix A – Supplementary Material

Additional supporting information was provided with graphic representation of preliminary studies, stability testing and accuracy assessment (Pearson plotting of the comparison with reference procedure). (ESM\_Ferreira\_et\_al.docx)

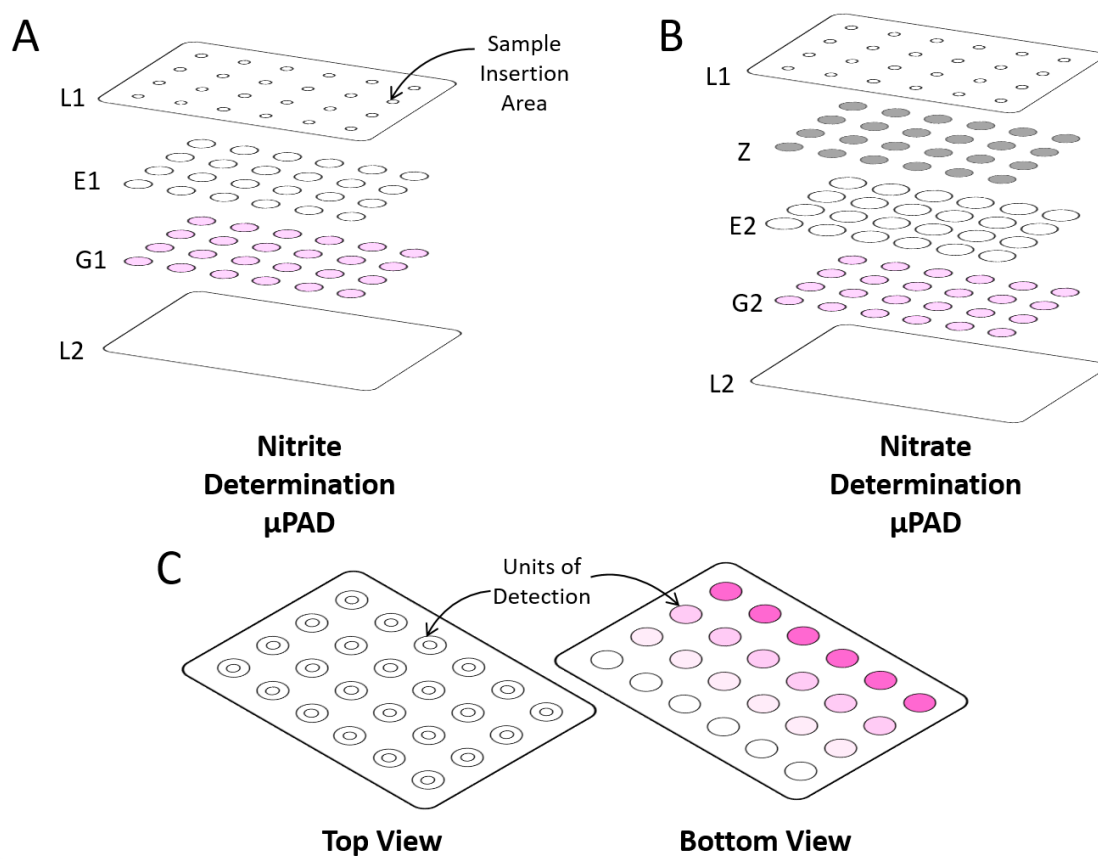
### References

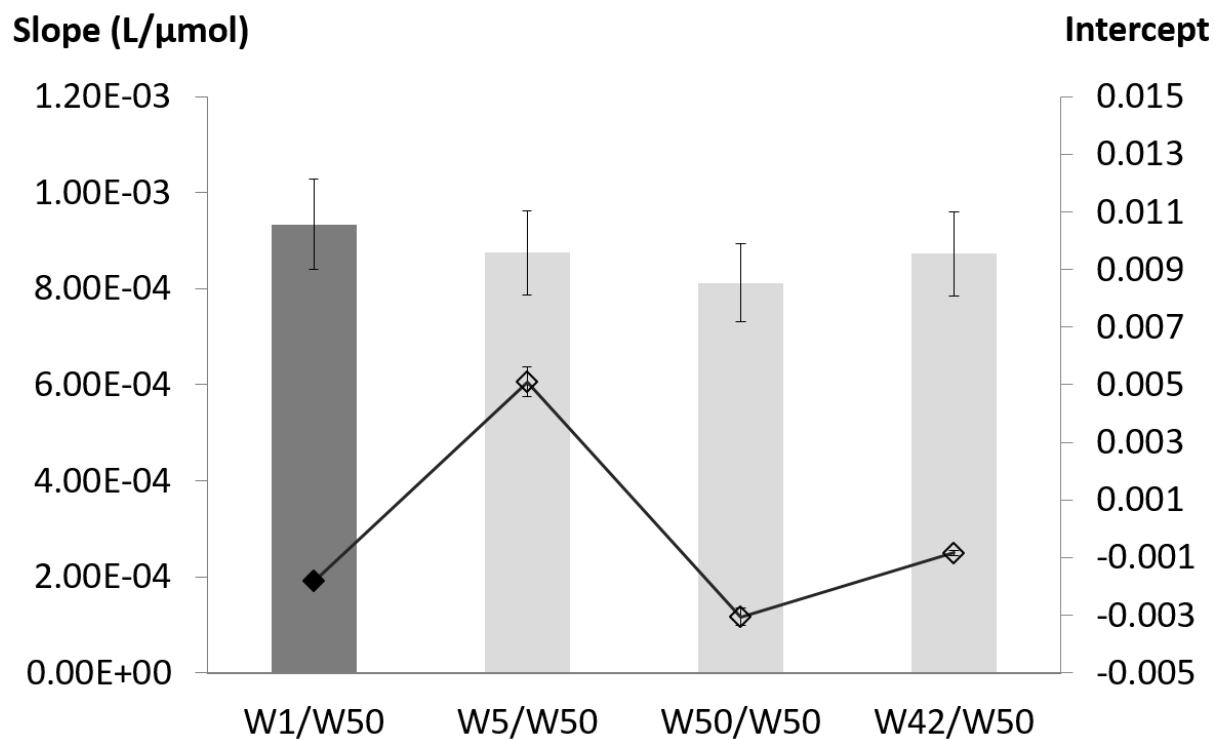
- [1] World Health Organization, Standing up for the right to health, (2018). <https://www.who.int/news-room/feature-stories/detail/standing-up-for-the-right-to-health> (accessed February 22, 2019).
- [2] C.A. Petti, C.R. Polage, T.C. Quinn, A.R. Ronald, M.A. Sande, Laboratory Medicine in Africa: A Barrier to Effective Health Care, *Clin. Infect. Dis.* 42 (2006) 377–382. <https://doi.org/10.1086/499363>.
- [3] R. McNerney, Diagnostics for Developing Countries, *Diagnostics*. 5 (2015) 200. <https://doi.org/10.3390/DIAGNOSTICS5020200>.
- [4] X. Jiang, Z.H. Fan, Fabrication and Operation of Paper-Based Analytical Devices, *Annu. Rev. Anal. Chem.* 9 (2016) 203–222. <https://doi.org/10.1146/annurev-anchem-071015-041714>.
- [5] C.S. Kosack, A.-L. Page, P.R. Klatser, A guide to aid the selection of diagnostic tests, *Bull. World Health Organ.* 95 (2017) 639–645. <https://doi.org/10.2471/BLT.16.187468>.
- [6] Paper microfluidic devices : A review 2017 - Elveflow, (n.d.). <https://www.elveflow.com/microfluidic->

- tutorials/microfluidic-reviews-and-tutorials/paper-microfluidic-devices-a-review-2017/ (accessed December 13, 2018).
- [7] A.W. Martinez, S.T. Phillips, M.J. Butte, G.M. Whitesides, Patterned Paper as a Platform for Inexpensive, Low-Volume, Portable Bioassays, *Angew. Chemie.* 119 (2007) 1340–1342. <https://doi.org/10.1002/ange.200603817>.
- [8] M.I.G.S. Almeida, B.M. Jayawardane, S.D. Kolev, I.D. McKelvie, Developments of microfluidic paper-based analytical devices ( $\mu$ PADs) for water analysis: A review, *Talanta.* 177 (2018) 176–190. <https://doi.org/10.1016/J.TALANTA.2017.08.072>.
- [9] A.W. Martinez, S.T. Phillips, G.M. Whitesides, E. Carrilho, Diagnostics for the developing world: Microfluidic paper-based analytical devices, *Anal. Chem.* 82 (2010) 3–10. <https://doi.org/10.1021/ac9013989>.
- [10] N.C. Birch, D.F. Stickle, Example of use of a desktop scanner for data acquisition in a colorimetric assay, *Clin. Chim. Acta.* 333 (2003) 95–96. [https://doi.org/10.1016/S0009-8981\(03\)00168-2](https://doi.org/10.1016/S0009-8981(03)00168-2).
- [11] A.N. Ramdzan, M.I.G.S. Almeida, M.J. McCullough, S.D. Kolev, Development of a microfluidic paper-based analytical device for the determination of salivary aldehydes, *Anal. Chim. Acta.* 919 (2016) 47–54. <https://doi.org/10.1016/j.aca.2016.03.030>.
- [12] J.O. Lundberg, E. Weitzberg, J.A. Cole, N. Benjamin, Nitrate, bacteria and human health, in: *Nat. Rev. Microbiol.*, Nature Publishing Group, 2004: pp. 593–602. <https://doi.org/10.1038/nrmicro929>.
- [13] M.J. Moorcroft, J. Davis, R.G. Compton, Detection and determination of nitrate and nitrite: a review, *Talanta.* 54 (2001) 785–803. [https://doi.org/10.1016/S0039-9140\(01\)00323-X](https://doi.org/10.1016/S0039-9140(01)00323-X).
- [14] S.R. Tannenbaum, A.J. Sinskey, M. Weisman, W. Bishop, Nitrite in Human Saliva. Its Possible Relationship to Nitrosamine Formation<sup>23</sup>, *JNCI J. Natl. Cancer Inst.* 53 (1974) 75–784. <https://doi.org/10.1093/jnci/53.1.79>.
- [15] S.S. Mirvish, K.J. Reimers, B. Kutler, S.C. Chen, J. Haorah, C.R. Morris, A.C. Grandjean, E.R. Lyden, Nitrate and nitrite concentrations in human saliva for men and women at different ages and times of the day and their consistency over time., *Eur. J. Cancer Prev.* 9 (2000) 335–42. <https://doi.org/10.1097/00008469-200010000-00008>.
- [16] Atsdr, Toxicological Profile for Nitrate and Nitrite, n.d. <https://www.atsdr.cdc.gov/ToxProfiles/tp204-c3.pdf> (accessed September 25, 2018).
- [17] B.M. Jayawardane, I.D. McKelvie, S.D. Kolev, Development of a gas-diffusion microfluidic paper-based analytical device ( $\mu$ PAD) for the determination of ammonia in wastewater samples, *Anal. Chem.* 87 (2015) 4621–4626. <https://doi.org/10.1021/acs.analchem.5b00125>.
- [18] P. Kerkar, What is Blue Baby Syndrome & How is it Treated?, (2018).

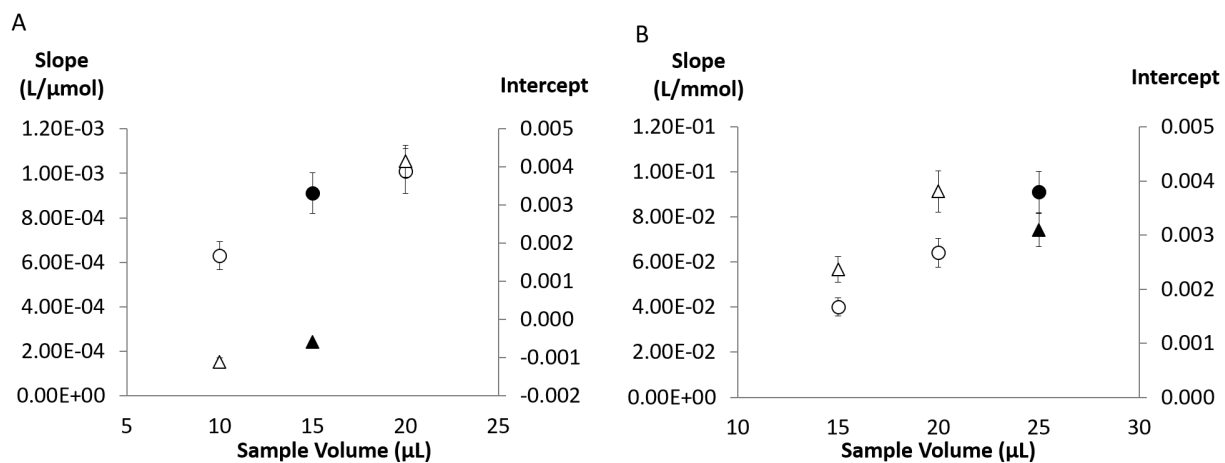
- <https://www.epainassist.com/blood-diseases/what-is-blue-baby-syndrome-and-how-is-it-treated>  
(accessed May 25, 2018).
- [19] G.A. Sánchez, V.A. Miozza, A. Delgado, L. Busch, Total salivary nitrates and nitrites in oral health and periodontal disease, *Nitric Oxide*. 36 (2014) 31–35. <https://doi.org/10.1016/J.NIOX.2013.10.012>.
- [20] J.J. Doel, M.P. Hector, C. V. Amirtham, L.A. Al-Anzan, N. Benjamin, R.P. Allaker, Protective effect of salivary nitrate and microbial nitrate reductase activity against caries, *Eur. J. Oral Sci.* 112 (2004) 424–428. <https://doi.org/10.1111/j.1600-0722.2004.00153.x>.
- [21] L.F. Hofman, Human Saliva as a Diagnostic Specimen, *J. Nutr.* 131 (2001) 1621S–1625S. <https://doi.org/10.1093/jn/131.5.1621S>.
- [22] S. Chojnowska, T. Baran, I. Wilińska, P. Sienicka, I. Cabaj-Wiater, M. Knaś, Human saliva as a diagnostic material, *Adv. Med. Sci.* 63 (2018) 185–191. <https://doi.org/10.1016/J.ADVMS.2017.11.002>.
- [23] M. Tiwari, Science behind human saliva, *J. Nat. Sci. Biol. Med.* 2 (2011) 53–58. <https://doi.org/10.4103/0976-9668.82322>.
- [24] S. Chiappin, G. Antonelli, R. Gatti, E.F. De Palo, Saliva specimen: A new laboratory tool for diagnostic and basic investigation, *Clin. Chim. Acta.* 383 (2007) 30–40. <https://doi.org/10.1016/J.CCA.2007.04.011>.
- [25] E.A. Almeida, P.D.V, Saliva Composition and Functions: A Comprehensive Review, *J. Comtemporary Dent. Pract.* Vol. 9. 9 (2008) 72–80.
- [26] G. Eisenbrand, B. Spiegelhalder, R. Preussmann, Nitrate and nitrite in saliva., *Oncology*. 37 (1980) 227–31. <https://doi.org/10.1159/000225441>.
- [27] C.F.C.P. Teixeira, R.L.A. Segundo, A.O.S.S. Rangel, R.B.R. Mesquita, M.T.S.O.B. Ferreira, A.A. Bordalo, Development of a sequential injection system for the determination of nitrite and nitrate in waters with different salinity: Application to estuaries in NW Portugal, *Anal. Methods*. 1 (2009) 195–202. <https://doi.org/10.1039/b9ay00101h>.
- [28] APHA, AWWA, WEF, Standard Methods for the Examination of Water and Wastewater, 20th ed., Washington, DC, 1998.
- [29] B.M. Jayawardane, S. Wei, I.D. McKelvie, S.D. Kolev, Microfluidic Paper-Based Analytical Device for the Determination of Nitrite and Nitrate, *Anal. Chem.* 86 (2014) 7274–7279. <https://doi.org/10.1021/ac5013249>.
- [30] A. Wiegand, G.R. Batista, C.R.G. Torres, B. Sener, T. Attin, Artificial Saliva Formulations versus Human Saliva Pretreatment in Dental Erosion Experiments, *Caries Res.* 50 (2016) 78–86. <https://doi.org/10.1159/000443188>.

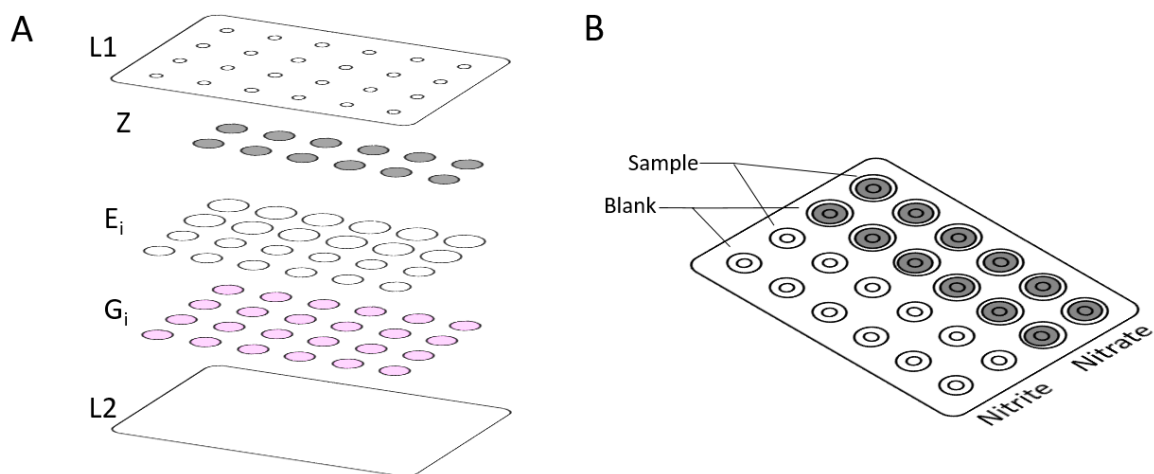
- [31] L.A. Currie, Nomenclature in evaluation of analytical methods including detection and quantification capabilities (IUPAC Recommendations 1995), *Pure Appl. Chem.* 67 (1995) 1699–1723. <https://doi.org/10.1351/pac199567101699>.
- [32] D.T. Burns, K. Danzer, A. Townshend, Use of the term “recovery” and “apparent recovery” in analytical procedures (IUPAC Recommendations 2002), *Pure Appl. Chem.* 74 (2002) 2201–2205. <https://doi.org/10.1351/pac200274112201>.
- [33] C.-K. Chiang, A. Kurniawan, C.-Y. Kao, M.-J. Wang, Single step and mask-free 3D wax printing of microfluidic paper-based analytical devices for glucose and nitrite assays, *Talanta*. 194 (2019) 837–845. <https://doi.org/10.1016/j.talanta.2018.10.104>.
- [34] E. Vidal, A.S. Lorenzetti, A.G. Lista, C.E. Domini, Micropaper-based analytical device ( $\mu$ PAD) for the simultaneous determination of nitrite and fluoride using a smartphone, *Microchem. J.* 143 (2018) 467–473. <https://doi.org/10.1016/j.microc.2018.08.042>.
- [35] Y.-C. Liu, C.-H. Hsu, B.-J. Lu, P.-Y. Lin, M.-L. Ho, Determination of nitrite ions in environment analysis with a paper-based microfluidic device, *Dalt. Trans.* 47 (2018) 14799–14807. <https://doi.org/10.1039/C8DT02960A>.
- [36] X.X. Zhang, Y.Z. Song, F. Fang, Z.Y. Wu, Sensitive paper-based analytical device for fast colorimetric detection of nitrite with smartphone, *Anal. Bioanal. Chem.* (2018) 1–5. <https://doi.org/10.1007/s00216-018-0965-2>.
- [37] Y. Jiang, Z. Hao, Q. He, H. Chen, A simple method for fabrication of microfluidic paper-based analytical devices and on-device fluid control with a portable corona generator, *RSC Adv.* 6 (2016) 2888–2894. <https://doi.org/10.1039/c5ra23470k>.
- [38] I. Ortiz-Gomez, M. Ortega-Muñoz, A. Salinas-Castillo, J.A. Álvarez-Bermejo, M. Ariza-Avidad, I. de Orbe-Payá, F. Santoyo-Gonzalez, L.F. Capitan-Vallvey, Tetrazine-based chemistry for nitrite determination in a paper microfluidic device, *Talanta*. 160 (2016) 721–728. <https://doi.org/10.1016/j.talanta.2016.08.021>.
- [39] B. Wang, Z. Lin, M. Wang, Fabrication of a paper-based microfluidic device to readily determine nitrite ion concentration by simple colorimetric assay, *J. Chem. Educ.* 92 (2015) 733–736. <https://doi.org/10.1021/ed500644m>.
- [40] T.M.G. Cardoso, P.T. Garcia, W.K.T. Coltro, Colorimetric determination of nitrite in clinical, food and environmental samples using microfluidic devices stamped in paper platforms, *Anal. Methods*. 7 (2015) 7311–7317. <https://doi.org/10.1039/c5ay00466g>.

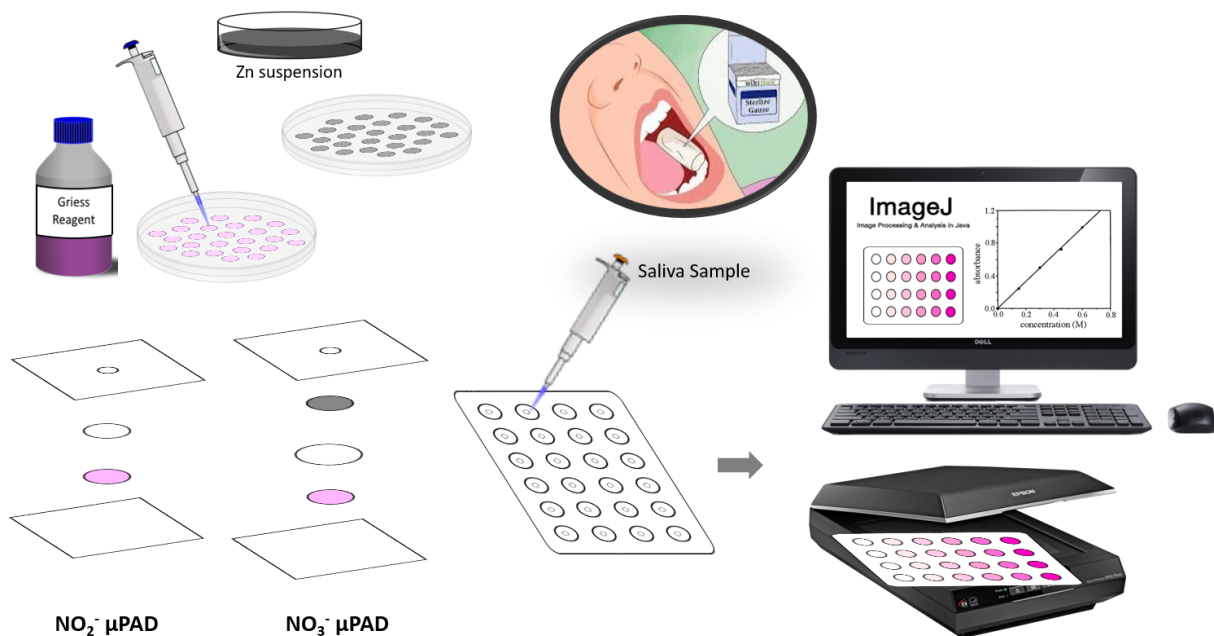












## **Research highlights**

- Design of the first  $\mu$ PAD for nitrite and nitrate determination in human saliva
- Nitrate reduction carried out within the novel device
- Direct saliva introduction, no sample pretreatment required
- Successfully applied to saliva samples collected from healthy volunteers

## Novel microfluidic paper-based analytical devices ( $\mu$ PADs) for the determination of nitrate and nitrite in human saliva

Francisca T. S. M. Ferreira, Raquel B. R. Mesquita\*, António O. S. S. Rangel

*Universidade Católica Portuguesa, CBQF - Centro de Biotecnologia e Química Fina – Laboratório Associado, Escola Superior de Biotecnologia, Rua Diogo Botelho 1327, 4169-005 Porto, Portugal*

*\*rmesquita@porto.ucp.pt*

### Abstract

In this work, two different microfluidic paper-based analytical devices ( $\mu$ PADs) were developed for the quantification of nitrite and nitrate in human saliva samples, in order to aid in the diagnosis of some diseases and health conditions associated with these ions. The development of these nitrite and nitrate  $\mu$ PADs involved several studies to optimize their design and construction, including an interference assessment and stability studies. These  $\mu$ PADs allowed a nitrite determination in a range of 5 - 250  $\mu$ M with limits of detection and quantification of 0.05  $\mu$ M and 0.17  $\mu$ M, respectively, and a nitrate determination in the range 0.2 – 1.2 mM with limits of detection and quantification of 0.08 mM and 0.27 mM, respectively. As for the stability, both of the  $\mu$ PADs were stable when stored in vacuum at 4°C (the nitrite  $\mu$ PAD for at least 60 days and the nitrate  $\mu$ PAD for at least of 14 days) and, after the sample placement, the nitrite and nitrate  $\mu$ PADs could be scanned within the first 4 and 2 hours, respectively. The nitrite  $\mu$ PAD measurements were compared with the ones obtained from the standard colorimetric method and there were no statistically significant differences between these two methods. To evaluate the accuracy of nitrate  $\mu$ PAD measurements, 4 certified water samples were used and recovery studies using saliva samples were performed.

**KEYWORDS:** *nitrite determination; nitrate reduction; saliva analysis; point-of-care; disposable devices*

## 1. Introduction

According to the World Health Organization, “more people can access essential health services today than ever before, but at least half of the world’s population still go without” the basic health care [1]. Even with the advances in technologies, there is still a lack of practical and affordable devices that can perform diagnosis and treatments on location, whether it might be in a medical institution, in the patients’ homes or in the most secluded areas [2,3]. That is why researchers have been working towards the development of new diagnostic and treatment devices and techniques that are “ASSURED”: Affordable, Sensitive, Specific, User-friendly, Rapid and robust, Equipment-free, and Deliverable to end-users [4,5].

In 2007, Martinez A. et al. introduced the concept of microfluidic paper-based analytical device, or  $\mu$ PAD, as a “platform for inexpensive, low-volume, portable bioassays” [6,7]. This type of devices is based on the presence of two different areas: a hydrophilic area provided by the paper where a reaction (usually colorimetric) occurs, and a hydrophobic area that delimits this reaction zone [4,8]. The most common design approach is wax printing, because it is a simple, and relatively fast method compatible with most  $\mu$ PAD applications [4,6]. Nevertheless, this type of printing method requires expensive wax and an extra step of heating in the process. The appeal of the use of paper as a reaction tool is justified not only by the paper’s low cost and high availability, but also by the fact that it is light weighted, available in several thicknesses and porosities, easy to store and transport, and compatible with biological samples (because of its cellulose matrix) [9]. With colorimetric reactions, the most commonly used detection method, the results can be easily interpreted visually or captured with digital cameras, mobile phones or portable scanners [6,8]. Then the color intensities can be obtained from the digital images by using image processing programs and converted in absorbance values [8,10]. A disadvantage of these detection methods is the high variability caused by a non-uniform distribution of the colored product in the paper, but this problem can be reduced by using more replicas and excluding outliers, if necessary [8].

The  $\mu$ PADs popularity is due to their various advantages. They are simple, portable, affordable, rapid, disposable, and, after being assemble, don’t require complex equipment or specialized personal to do the measurement, which makes them and interesting tool to be used in on-site analysis in locations of difficult access or with very few resources [11]. However, very few of the developed  $\mu$ PADs reported so far, presented any on-field or stability studies [3,8].

Nitrite and nitrate are nitrous acid salts found in the human body due to either an endogenous produce in the body or ingestion through food and water [12,13]. For many years these ions have been associated with cancer, especially nitrite, either from direct ingestion, or the nitrate reduction by bacteria in human saliva. When nitrite reaches the acidic environment of the stomach, and combined with amine or amide, it forms nitrosamines and nitrosamides, which are toxic and carcinogenic, thus contributing mainly to the

development of gastric cancer [13–15]. When absorbed to the bloodstream, nitrite can react with the iron in hemoglobin, irreversibly converting it in methemoglobin and preventing it from carrying oxygen (methemoglobinemia) [13,16–18]. Even though NO<sub>x</sub> compounds have been associated with cancer and other diseases since 1970s, recently a few studies have been reporting newly found benefits of these ions. Salivary nitrates and nitrites may not only be a defense response to oral infectious diseases like periodontal disease [19], but also present a protective effect against dental caries [20].

Several methods have been described for nitrite and nitrate determination, but these methods have some limitations like requiring high volume of reagents and sample, the time of analysis, the use of complex lab equipment, the need of constant power, specialized technicians, the production of toxic waste, among others. These limitations can be emphasized when targeting biological fluids. The most common biological fluid used as samples is blood/serum. However, this type of sample demands an invasive collection procedure with a considerable discomfort to the patient and requiring specialized personnel, very specific storage conditions, together with a risk of contamination and of spreading diseases [21,22]. So, in the last few years there has been an increase in targeting other biological fluids, such as urine and saliva.

The collection of saliva is easier, safer and more economic when compared with blood collection [22–24]. Additionally, it is a painless noninvasive procedure, with a lower risk of contamination or dispersion of contagious diseases [22,23], which does not require specialized medical personnel, and it can be done in secluded areas and more often than the blood collection [21–23]. As a sample, saliva has been known to contain several substances of interest for screening and diagnosis purposes and, although is preferable to be kept on ice, the samples are stable for 24 h at room temperature or for a week at 4°C [11,21,22]. Besides, for some groups of patients, like children, seniors or, for example, patients with blood clotting disorders, it would be easier to collect saliva [22,24]. However, it also has some disadvantages. One of the big issues of using this fluid as a sample is the lack of specific information on biomarkers concentrations in saliva, mainly because it is a very recent and new approach [21,23]. Another problem can be the variations in its composition that can occur according to some factors: age, gender, the time of the day of the sample collection and if it was or not stimulated [15,25]. The mean salivary nitrite and nitrate in humans, according to recent studies, was found to be approximately between 1 - 10 mg/L and 10 - 80 mg/L, respectively [12,19,26].

The focus of this work was to develop two new microfluidic paper-based analytical devices ( $\mu$ PADs) for the quantification of nitrite and nitrate anions in human saliva samples, using a new construction approach that has not been reported yet, and based on the Griess reaction for spectrophotometric detection. The idea was for these  $\mu$ PADs to ultimately be capable of being used as a screening option not only in healthcare facilities, but also to aid in the diagnosis of some diseases and health conditions in remote locations.

## 2. Materials and methods

### 2.1. Reagents and solutions

The solutions used in this work were prepared with analytical grade chemicals and Milli-Q water, (resistivity  $> 18 \text{ M}\Omega/\text{cm}$ , Millipore, USA).

The standard stock solution of 13 mM sodium nitrite (Merck) was monthly prepared by dissolving approximately 20 mg of the previously dried (overnight  $100^\circ\text{C}$ ) solid in 25 mL of water. A fivefold dilution of sodium nitrite stock solution (2.5 mM) was weekly made in order to prepare, also weekly, the working standards of nitrite in the range of 5 - 250  $\mu\text{M}$ .

The standard stock solution of 12 mM sodium nitrate (Merck) was prepared monthly by dissolving approximately 50 mg of the previously dried (overnight  $100^\circ\text{C}$ ) in 50 mL of water. The working nitrate standards were prepared daily from the standard stock solution in a range of 0.2 - 1.2 mM.

The Griess reagent was monthly prepared according to Mesquita R. et al. [27] by dissolving approximately 0.4 g of sulfanilamide (Sigma-Aldrich) in 2 mL of 5 M orthophosphoric acid and 0.04 g of N-(1-naphthyl)-ethylenediamine dihydrochloride (N1NED) (Merck) in water. These two homogenized solutions were mixed together, and the volume was completed to 20 mL. This solution was stored in a dark bottle and shielded from the light.

A zinc suspension was prepared for every 4  $\mu\text{PADs}$  (maximum), by mixing 1 g of zinc powder ( $<10 \mu\text{m}$ ) (Sigma-Aldrich) in 20 mL of water.

### 2.2 Design of the developed $\mu\text{PADs}$

The assembly of both  $\mu\text{PADs}$  consisted in aligning twenty-four sets of filter paper disks (hydrophilic area) in a 4 columns and 6 rows' distribution, under previously perforated 4 mm holes (for the sample insertion) (L1) made in a 75x110 mm plastic laminating pouch (Q-Connect) (hydrophobic area) (Fig. 1).

The nitrite determination  $\mu\text{PAD}$  consisted of two layers: E1 (Whatman Grade 1 filter paper 9.5 mm diameter empty disk) and G1 (Whatman Grade 50 filter paper 9.5 mm diameter disk with 5  $\mu\text{L}$  of the Griess reagent added and left to dry in a  $50^\circ\text{C}$  oven for 10 minutes), as shown in Fig. 1A.

The  $\mu\text{PAD}$  for nitrate determination consisted of three different sizes and types of paper aligned over each other (Fig. 1B): the top layer Z (Whatman Grade 1 filter paper, 9.5 mm diameter disk embedded in a zinc suspension with a 30 seconds manual agitation and left to dry in a  $50^\circ\text{C}$  oven for approximately 30 minutes), the layer E2 (Whatman Grade 1 filter paper, 1.27 cm diameter empty disk), and the bottom layer G2 (Whatman Grade 50 filter paper, 9.5 mm diameter disk with 10  $\mu\text{L}$  of the Griess reagent added and left



to dry in a 50°C oven for 10 minutes). After the alignment, the laminating pouches passed through the pouch laminator (Fellowes L125 - A4), which allow the plastic pouch to melt and seal around the paper filter disks, thus creating a strong physical barrier between the units of detection (Fig. 1C). After the lamination, the  $\mu$ PADs were ready to be used.

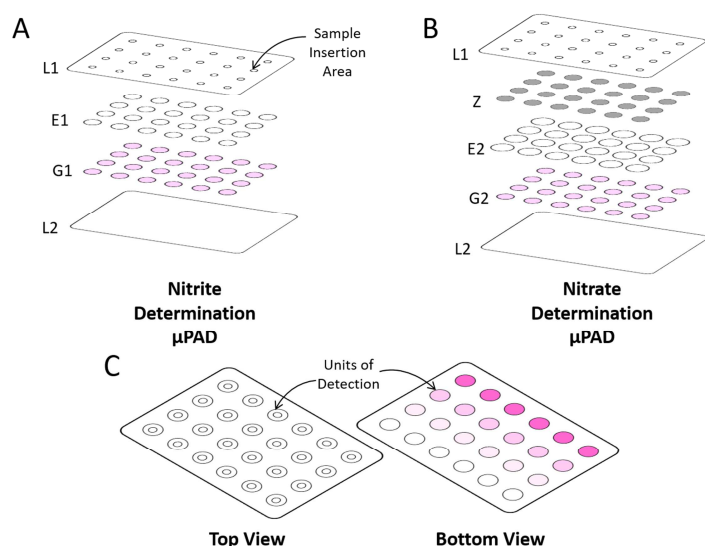


**Fig. 1.** Schematic assembly of the  $\mu$ PAD for the nitrite (A) and nitrate (B) determination and the schematic representation of the device after sample placement; (C); L1, top layer of the laminating pouch; L2, bottom layer of the laminating pouch; E1, empty layer; G1, Griess reagent layer (5  $\mu$ L per disk); Z, zinc embedded layer; E2, empty layer; G2, Griess reagent layer (10  $\mu$ L per disk).

### 2.3. Determination procedure for NO<sub>x</sub> determination

After the  $\mu$ PADs assembly, to perform the measurements, 15  $\mu$ L and 25  $\mu$ L of sample/standard were injected in each sample insertion hole of the  $\mu$ PADs for nitrite and nitrate determination, respectively. When the sample was completely absorbed, the holes were covered with adhesive tape in order to prevent evaporation of the sample and possible contaminations. The sample/standard flows through the layers L1/E1/G1 and L1/Z/E2 (nitrite and nitrate, respectively) until it reacts with the Griess reagent (layer G1/G2), forming a pink color product in which the intensity of the shade of pink is directly proportional to the concentration of nitrite or NO<sub>x</sub> (in the case of the nitrate  $\mu$ PAD) in the sample (Fig. 1C).

In order to measure the intensity of the color, the bottom layer of the  $\mu$ PADs were scanned using a standard scanner (Canon LiDE 120) and the images were processed using ImageJ (National Institutes of

Health, USA). In this work, the scanning time was considered the period of time between the sample/standard introduction and the scanning of the  $\mu$ PAD.

In the ImageJ, the images were converted into RGB plots. Since the expected colored product of the Griess reaction is pink and the complementary color in which this product absorbs is the green one, the green filter of the RGB plots was used to measure the intensity of pink in the images. For each color disk, an option was made to do the measurements with the circular selection tool with 200x200 pixels, because it allowed better adjustment to the reagent disk area (9.5 mm diameter).

As Birch and Stickle described [10], measured intensities of pink were converted in absorbance values using the formula:  $A = \log_{10}(I_B/I_S)$ , where  $A$  is the absorbance value,  $I_S$  is the average measured intensity (of the pixels) of the standard or sample, and  $I_B$  is the average measured intensity (of the pixels) of the blank. In order to remove outliers, 4 out of the 6 intensity measurements obtained were used in the average calculations.

Regarding the determination of nitrate, the value obtained corresponds in fact to the sum of the content of nitrate plus nitrite ( $\text{NO}_x$ ). However, as the nitrite values in saliva are much lower than those of nitrite, no need for subtraction is needed.

#### 2.4. Reference procedures - accuracy assessments

In order to assess the accuracy of  $\mu$ PAD measurements and to validate the developed  $\mu$ PAD for the nitrite determination, a comparison was made between the  $\mu$ PAD measurements and the results obtained by the reference procedure for water analysis [28] since there are no reference methods for saliva analysis. All the solutions used were also prepared accordingly.

As no certified saliva samples are available, a certified water sample was used, QC RW1 (VKI reference materials, DANAK) to assess the accuracy of the nitrate  $\mu$ PAD measurements. This water sample consisted of one ampoule with a concentrate for preparation of reference sample by dilution with water. Therefore, 4 rigorous dilutions were prepared, and the final  $\text{NO}_x$  concentrations were 0.707 mM (CWS\_1), 0.530 mM (CWS\_2), 0.471 mM (CWS\_3) and 0.354 mM (CWS\_4). Recovery percentages were also calculated for human saliva samples, to which a known concentration of nitrate was added.

#### 2.5. Saliva samples collection

The saliva samples used in this work were all collected from healthy volunteers in a range of 20 to 40 years, with their informed consent, by placing a 5x5 cm sterile gauze (Wells) in the mouth for approximately two minutes. The gauze was then placed in a 5 mL sterile syringe and squeezed in order to remove

the saliva from the gauze to a 5 mL plastic tube. These samples were diluted to half and were either used immediately (as fresh samples) or stored at -20°C for later use (frozen samples).

### 3. Results and discussions

#### 3.1. Preliminary studies

As already mentioned, the Griess reaction is perhaps the most commonly known and used reaction for the determination of nitrite. However, there are several ways to prepare the Griess reagent. So, in order to obtain the best sensitivity possible, two compositions of the reagent were tested, both in a batchwise procedure and in filter paper: one reported by Mesquita et al. [27], reagent A (116 mM of sulfanilamide; 500 mM of *ortho*-phosphoric acid; 8 mM of N1NED), and the other by Jayawardane et al. [29], reagent B (50 mM of sulfanilamide; 330 mM of citric acid; 10 mM of N1NED). The chosen reagent was the reagent A, since it presented a higher sensitivity, not only in the batchwise procedure but also on paper (ESM Fig. 1).

As for the nitrate determination, in order to use the same reaction, it was necessary to reduce nitrate to nitrite. Three known reducing agents, namely hydroxylamine, ascorbic acid and tin chloride, were tested alongside with the Griess reagent in a batchwise procedure. However, there was no formation of the expected pink color, which indicated that neither of the tested reagents were able to extensively reduce nitrate to nitrite. So, it was necessary to consider an alternative; zinc has been reported by Jayawardane et al. (2014) [29] to be a powerful reducing agent capable of this conversion. So, a batchwise procedure with the Griess reagent and a Zn powder (<10 µm; Sigma-Aldrich) was prepared and the results confirmed that zinc was an effective reducing agent for nitrate.

#### 3.2. Nitrite determination

After testing the reaction in a batchwise procedure and in paper, the next step was to design the µPAD for nitrite determination. Having set the physical structure of the µPAD to use a plastic laminating pouch as the hydrophobic area, and filter paper discs for the hydrophilic areas, (24 filter paper disks were used to attain 24 units of detection per µPAD) the filter paper layers were studied.

Since there is only one reagent for the nitrite determination, a µPAD with only one layer of filter paper disks containing the Griess reagent was prepared, corresponding to the G1 in Fig. 1A. However, because the reagent was in direct contact with the air through the sample insertion hole, it oxidized very easily. Moreover, one layer allowed a very limited volume of sample (10 µL maximum) and it took a long time to absorb that same volume (30 minutes minimum for 10 µL). So, an empty layer (with no reagent) was added on top of the reagent layer (E1 in Fig. 1A) in order to try to protect it from oxidation and also to allow

the placement of a higher volume of sample with a smaller absorption time. In this 2-layers  $\mu$ PAD, the same 10  $\mu$ L of sample was completely absorbed in less than 5 minutes.

Several types of filter paper with different treatments and pore diameters available were tested from Whatman® (ESM Table 1). For the reagent layer (G1 in Fig. 1A), the absorbance value obtained for a nitrite standard of 30  $\mu$ M was compared for different filter papers (Whatman Grade 1, 42, 50 and 541) using 10  $\mu$ L of reagent. The Whatman 50 (W50) paper was the one chosen, as it presented a higher absorbance value.

Then the filter paper of the empty layer (E1 in Fig. 1A) was studied by establishing calibration curves with different filter papers, namely Whatman Grade 1, 5, 42 and 50 together with the W50 paper in the reagent layer (G1 in Fig. 1A). The highest sensitivity, calibration curve slope, was obtained with Whatman Grade 1 (W1) in the empty layer (Fig. 2), together with one of the lowest intercepts (indicating a potentially lower detection limit) so that was the chosen filter paper. This combination of W1 for empty layer and W50 for reagent layer also enabled the  $\mu$ PAD scanning in least amount of time of all the papers studied (scanning in 20 minutes).

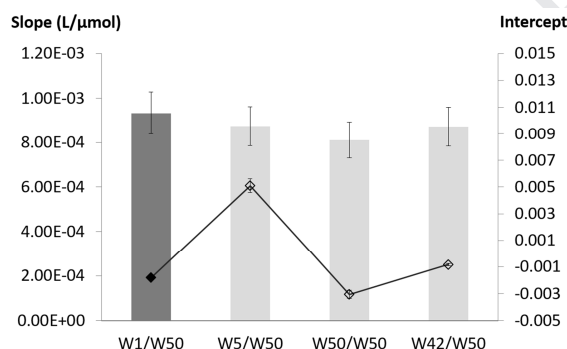


**Fig. 2.** Study of the influence in the calibration curve parameters, slope (grey bars) and intercept (diamonds) of different types of filter paper in the first layer on the nitrite determination  $\mu$ PAD; the chosen combination is represented by the dark grey and black diamond.

After setting the physical parameters, the volume of Griess reagent to place on the reagent layer  $\mu$ PAD was studied. In a preliminary test of the volume capacity of these paper disks, the reagent volumes studied were 5 and 10  $\mu$ L, since lower volumes would not distribute through the entire disk and higher volumes resulted in soaking the disk. Calibration curves were established for both of these volumes and it was possible to observe that there was no significant difference (<10%) between the sensitivities (nor the intercepts). So, to avoid the unnecessary consumptions of reagents, a volume of 5  $\mu$ L of Griess reagent per paper disk was chosen for the G1 layer of the nitrite  $\mu$ PAD.

The last parameter tested was the sample volume, and calibration curves were prepared with the standard volumes of 10, 15 and 20  $\mu\text{L}$  (Fig. 3A).

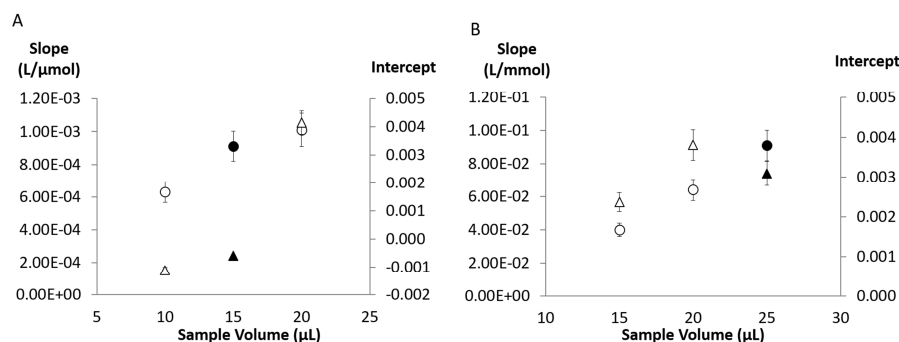


**Fig. 3.** Study of the influence of the reagent volume in the  $\mu\text{PADs}$  calibration curve slope (○) and intercept (Δ) for: A, the nitrite determination and B, the nitrate determination; the points in black represent the chosen values.

When using either 10 or 15  $\mu\text{L}$ , the sample was completely absorbed in approximately 15 minutes. When applying 20  $\mu\text{L}$  of sample, it took about 35 minutes for the  $\mu\text{PAD}$  to completely absorb that sample/standards. Although the highest sensitivity was achieved using the 20  $\mu\text{L}$  of sample, the chosen sample volume was the 15  $\mu\text{L}$ , as a compromise solution between sensitivity and scanning time.

### 3.3. Nitrate Determination.

After testing different reducing agents in a batchwise procedure and choosing zinc powder as the reducing agent (preliminary tests), the challenge became placing/immobilizing that powder in the filter paper.

The main concern was the paper low retention capacity and the uneven distribution of the zinc powder. Several procedures were tested, including passing a zinc suspension through the filter paper with a syringe, but the most efficient one consisted in placing the filter paper disks in a zinc suspension (1 g of zinc powder in 20 mL of water), stir the suspension manually and then set the disks to dry (50°C oven for 30 minutes). Therefore, for the nitrate  $\mu\text{PAD}$ , a two-layer assembly was tested, similar to the nitrite  $\mu\text{PAD}$ , but instead of the empty layer (E1 in Fig. 1A) there was the zinc suspension layer (Z layer in Fig. 1B).

However, the direct contact of the Z layer with the Griess reagent layer (G2 layer) caused a visible degradation of the reagent, even before the sample/standard insertion. So, in order to prevent the Griess reagent degradation, an empty layer of filter paper was added between the Z and G2 layers. To ensure that there was no contact, this extra layer (E2 in Fig. 1B) consisted in a W1 filter paper disk with a bigger di-

ameter (1.27 cm) than the other layers (0.95 cm). This approach effectively prevented the reagent degradation and defined the design of the nitrate  $\mu$ PAD with 3 layers (Fig. 1B).

The assembly of the nitrate  $\mu$ PAD consisted of detection sets with 3 layers of filter paper: W1, zinc suspension layer (Z in Fig. 1B); W1, empty bigger disk layer (E2 in Fig. 1B); W50, Griess reagent layer (G2 in Fig. 1B). As the targeted concentration range of nitrate was higher than the nitrite concentration range, the influence of the reagent volume was studied again. Calibration curves were set and the same volumes of 5 and 10  $\mu$ L were tested; 10  $\mu$ L of Griess reagent produced a 10% increase of the sensitivity, when compared with the 5  $\mu$ L. Therefore, the chosen volume to be used on the nitrate  $\mu$ PAD was 10  $\mu$ L of the Griess reagent.

Because a third layer of paper was introduced in the  $\mu$ PAD, the  $\mu$ PAD absorption capability increased significantly. Therefore, it was important to study the sample volume, and choose the volume that allows a higher sensitivity. So, calibration curves were made, and the sample volumes tested were 15, 20, 25 and 30  $\mu$ L. With the first three volumes, the sample was completely absorbed into the  $\mu$ PAD almost immediately, but when 30  $\mu$ L of sample was used, it took about 35 minutes to observe the sample absorption. Since, 35 minutes was considered too much time, the option of 30  $\mu$ L of sample was excluded from the study. For the remaining volumes, even though it was possible to scan the  $\mu$ PAD almost immediately after sample introduction, the sensitivities increased exponentially for the first 20 minutes. This can be due to the fact that the conversion of nitrate to nitrite slows down the color reaction. So, to compare the effect of the sample volume, a scanning time of 20 minutes was used (Fig. 3B). Out of the volumes tested, the calibration curve with the highest sensitivity was obtained with 25  $\mu$ L of sample, therefore it was the chosen volume.

In fact, the  $\mu$ PAD for nitrate determination attains the determination of both nitrate and nitrite in a  $\text{NO}_x$  quantification. This can be explained as any nitrite present goes through the zinc layer (Z in Fig. 1B) to the detection layer (G2 in Fig. 1B) producing the color product. Considering the difference in the expected concentration ranges for nitrite and nitrate, it is not expected to be a significant effect. However, due to the versatility of these devices, a  $\mu$ PAD for both determinations can be produced (Fig. 4) by assembling two of the four columns identically to the nitrite determination design (one for the introduction of the blank and one for the sample) and the other two columns identically to the nitrate (also one for the introduction of the blank and one for the sample). This mixed design allows the simultaneous determination of nitrite and nitrate ions using one  $\mu$ PAD per sample without compromising the number of replicas (6 detection units per column).

### 3.4. Interferences assessment

To study the interference of the saliva matrix, a set of the developed  $\mu$ PADs were prepared to perform two calibration curves for each determination, nitrite and nitrate using standards in water, and in synthetic saliva. The synthetic saliva prepared was based on the concentrations reported by Batista G. et al. [30] :  $[\text{KCl}] = 2237 \text{ mg/L}$ ;  $[\text{KH}_2\text{PO}_4] = 544.3 \text{ mg/L}$ ;  $[\text{HEPES}] = 4766 \text{ mg/L}$ ;  $[\text{CaCl}_2 \cdot 2\text{H}_2\text{O}] = 77.69 \text{ mg/L}$ ;  $[\text{MgCl}] = 19.04 \text{ mg/L}$ ;  $[\text{Bovine Serum Albumin}] = 2700 \text{ mg/L}$ .

For both nitrite and nitrate determination, the use of standards in a synthetic saliva matrix revealed no significant difference on the sensitivity of the calibration curves ( $< 10\%$ ). Therefore, to simplify the process and to reduce the reagents consumption, it was chosen to maintain the use of standards prepared in water, for both the nitrite and nitrate determinations.

### 2.3. Stability Studies

In order to evaluate the robustness of the developed  $\mu$ PADs, stability studies were designed and performed to test the stability of these microfluidic devices not only when stored, before the standard insertion, but also to evaluate the stability of the colored product formed after the standard insertion.

To evaluate the stability of colored product in both of the developed  $\mu$ PADs, a calibration curve for each determination, nitrite and nitrate, was prepared. The  $\mu$ PADs were scanned several times after the standards insertion, up to 4 hours (ESM Fig. 2). The results for the nitrite determination showed there is no significant difference ( $< 10\%$ ) between the sensitivity obtained when scanning the  $\mu$ PAD at 20 minutes or 4 hours after the standard insertion. As for the  $\mu$ PAD for nitrate determination initially there was an increase in the sensitivity, up until 1 hour. This can be explained not only by the existence of an extra layer, but also the existence of a reduction reaction before the color reaction, both of which slow down the formation of the colored product. After reaching a maximum slope (after 1 hour), the sensitivity begins to decrease up to the tested 4 hours. However, the initial increase of sensitivity was not statistically significant when considering a  $\pm 10\%$  range. Whereas, if the  $\mu$ PAD is scanned 3 hours or more after the standard/sample placement, the sensitivity obtained is significantly lower ( $> 18\%$ ) than the one obtained up until the 2 hours.

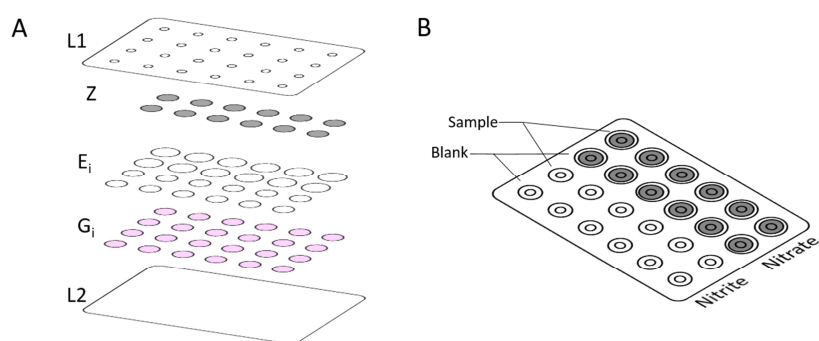


**Fig. 4.** Schematic assembly of the mixed  $\mu$ PAD for determination of both nitrite and nitrate ions; A, alignment; B, finished device.



To test the stability of the  $\mu$ PADs before the standard insertion, these devices were prepared and stored, always protected from light, under three different atmospheric conditions (air, nitrogen, and vacuum), both at room temperature (approximately 21°C) and refrigerated (approximately 4°C). The  $\mu$ PADs tested in air atmosphere were stored in a closed clear zip lock bag; the ones in nitrogen atmosphere were stored in a closed clear zip lock bag previously filled with nitrogen gas for approximately 1-2 minutes. The  $\mu$ PADs tested in a vacuum were also stored in a closed clear zip lock bag, in which the air was removed using a vacuum pump. All  $\mu$ PADs were shielded from the light when stored by covering in tin foil. Different periods of time were tested for each of the atmospheric condition. Every time the  $\mu$ PADs were removed from storage, a calibration curve was set. On the same day, another calibration curve was prepared using the same set of standards, on freshly assembled  $\mu$ PADs. The average sensitivity of these calibration curves was then compared with the sensitivities of the  $\mu$ PADs under the different conditions and a variation under 10% of the average calibration curves was considered non-significant (ESM Fig. 3).

The  $\mu$ PAD for nitrite determination was stable for 3 days for all three storage conditions at room temperature but only when kept in vacuum it was stable for 7 days. When stored in vacuum and refrigerated it was stable for at least 60 days. As for the  $\mu$ PAD for nitrate determination, it was possible to conclude that at the room temperature it was only stable with the storage in vacuum and only for 3 days. Neither the air atmosphere, nor the nitrogen atmosphere were able to appropriately preserve the  $\mu$ PAD for none of the periods of time tested, which is justified by the decrease of the calibration curves sensitivities below the acceptable  $\pm 10\%$  range. When stored in vacuum at fridge temperature, the  $\mu$ PADs for nitrate determination were stable for at least 14 days.

#### 2.4. Analytical features of the $\mu$ PAD for NO<sub>x</sub> determination

The main characteristics of the developed  $\mu$ PAD such as dynamic range, average calibration curve, limit of detection (LOD) and quantification (LOQ), relative standard deviation (RSD) and the  $\mu$ PADs optimal scanning time range, are summarized in Table 1.

Within the nitrite working concentration range 5 – 250  $\mu$ M, different sensitivities were observed, so this concentration range was divided in two, the range of 5 to 45  $\mu$ M and the range of 45 to 250  $\mu$ M. The limit of detection (LOD) and limit of quantification (LOQ) were calculated as concentration corresponding to three or ten-times, respectively, the standard deviation of the intercept, according to IUPAC recommendations [31].

The repeatability of the developed  $\mu$ PADs was evaluated calculating the relative standard deviation (RSD) obtained dividing the standard deviation of the calibration slope by the average of that slope.

**Table 1.** Features of the developed  $\mu$ PADs for the determination of nitrite and nitrate; Limit of Detection (LOD); Limit of Quantification (LOQ); Relative Standard Deviation (RSD).

Analyte	Dynamic range	Calibration Curve <sup>a</sup> $A = S \times [NO_x] + b$	LOD <sup>a</sup> ( $\mu$ M)	LOQ <sup>a</sup> ( $\mu$ M)	Repeatability, RSD <sup>b</sup>		Scanning Time
					Intraday	Interday	
Nitrite	5 – 45 $\mu$ M	$y = 1.78 \times 10^{-3} (\pm 5.60 \times 10^{-5}) \times [NO_2^-] + 1.12 \times 10^{-3} (\pm 3.08 \times 10^{-5})$ $R^2 = 0.997$	0.05	0.17	5%	2%	20 min – 4 h
	45 – 250 $\mu$ M	$y = 1.12 \times 10^{-3} (\pm 3.05 \times 10^{-5}) \times [NO_2^-] + 3.21 \times 10^{-2} (\pm 2.57 \times 10^{-3})$ $R^2 = 0.996$			2%	3%	
Nitrate	0.2 – 1.2 mM	$y = 7.27 \times 10^{-2} (\pm 8.35 \times 10^{-3}) \times [NO_3^-] - 2.63 \times 10^{-3} (\pm 1.93 \times 10^{-3})$ $R^2 = 0.988$	80	270	6%	5%	20 min – 2 h

<sup>a</sup> n=6; <sup>b</sup> n=4.

The intraday and interday repeatability were assessed performing 5 calibration curves in the same day and in consecutive days, respectively.

### 2.3. Application of the developed $\mu$ PADs - Accuracy Assessments

To assess the accuracy of the developed  $\mu$ PAD for nitrite determination, saliva samples were analyzed using the  $\mu$ PAD ( $[NO_2^-]_{\mu PAD}$ ) and with the reference method ( $[NO_2^-]_{Ref.Met.}$ ) [28] and the results compared (ESM Fig. 4A). The collected samples (#16) were all within the expected range of concentrations.

A linear relationship between the two set of results was established:  $[NO_2^-]_{\mu PAD} = 1.00(\pm 0.11) \times [NO_2^-]_{Ref.Method} - 2.74(\pm 6.82)$ . There was no statistical difference between the two methods, as the slope was not statistical different from 1 and the intercept was not statistically different from 0. To evaluate the accuracy of the developed  $\mu$ PAD for nitrate measurements, four dilutions of a certified water sample were used as the certified values were for  $NO_x$ , the same as the  $\mu$ PAD for nitrate determination (Table 2).

**Table 2.** Analysis of certified water samples performed with the nitrate determination  $\mu$ PAD; Standard deviation (SD); Relative deviation (RD)

Sample ID	$[NO_x]_{Found} \pm$	$[NO_x]_{Expekte}$	RD
-----------	----------------------	--------------------	----

	<b>SD (mM)</b>	<b>d (mM)</b>	<b>%</b>
<i>CWS_1</i>	0.681 ± 0.096	0.707	-3.6
<i>CWS_2</i>	0.526 ± 0.134	0.530	-0.7
<i>CWS_3</i>	0.393 ± 0.120	0.471	-16.7
<i>CWS_4</i>	0.328 ± 0.107	0.354	-7.2

A linear relationship between the two set of results was established (ESM Fig. 4B):  $[\text{NO}_2^-]_{\mu\text{PAD}} = 1.04(\pm 0.41) \times [\text{NO}_3^-]_{\text{Certified Value}} - 0.05(\pm 0.22)$ . There was no statistical difference between the certified value and the  $\mu\text{PAD}$  measurement, as the slope was not statistical different from 1 and the intercept was not statistically different from 0.

To further assess the accuracy of the nitrate measurements recovery studies were performed by spiking the samples with 4  $\mu\text{L}$  and 8  $\mu\text{L}$  of the nitrate standard stock solution to 1 mL of the saliva sample, and the calculation of the recovery percentage was made according to IUPAC [32], amount found minus the initial amount over the amount added (Table 3).

**Table 3.** Recovery studies performed with spiked human saliva samples assessed with the developed  $\mu\text{PAD}$  for nitrate determination; Standard deviation (SD); Relative standard deviation (RSD).

<b>Sample ID</b>	<b>Initial</b>			<b><math>[\text{NO}_3^-]_{\text{Added}}</math> (mM)</b>	<b>Found</b>			<b>Recovery (%)</b>
	<b><math>[\text{NO}_x]_{\text{Initial}}</math> (mM)</b>	<b>SD</b>	<b>RSD (%)</b>		<b><math>[\text{NO}_x]_{\text{Found}}</math> (mM)</b>	<b>SD</b>	<b>RSD (%)</b>	
<i>SS_1</i>	0.434	0.053	12%	0.216	0.627	0.052	8%	90
<i>SS_2</i>	0.434	0.053	12%	0.431	0.844	0.206	24%	95
<i>SS_3</i>	0.487	0.019	4%	0.216	0.699	0.221	32%	98
<i>SS_4</i>	0.487	0.019	4%	0.431	0.895	0.243	27%	95
<i>SS_5</i>	0.372	0.044	12%	0.216	0.593	0.095	16%	103
<i>SS_6</i>	0.372	0.044	12%	0.431	0.822	0.102	12%	104
<i>SS_7</i>	0.509	0.059	12%	0.216	0.713	0.108	15%	95
<i>SS_8</i>	0.609	0.081	13%	0.431	1.068	0.166	16%	106
<i>SS_9</i>	0.384	0.101	26%	0.216	0.612	0.082	13%	106
<i>SS_10</i>	0.384	0.101	26%	0.431	0.791	0.081	10%	94
<i>SS_11</i>	0.491	0.086	18%	0.216	0.701	0.205	29%	97
<i>SS_12</i>	0.491	0.086	18%	0.431	0.932	0.094	10%	102
<i>SS_13</i>	0.621	0.054	9%	0.216	0.825	0.157	19%	94
<i>SS_14</i>	0.275	0.053	19%	0.216	0.486	0.106	22%	98

<i>SS_15</i>	0.275	0.053	19%	0.431	0.694	0.080	12%	97
--------------	-------	-------	-----	-------	-------	-------	-----	----

The average of the calculated recoveries was 98% with a standard deviation of 5%. A statistical test (t-test) was used to evaluate if the mean recovery value did significantly differ from 100%. For a 95% significance level the calculated t-value was 1.32 with a correspondent critical value of 2.51. The statistical results indicate the absence of multiplicative matrix interferences proving that the developed  $\mu$ PAD was applicable to saliva samples.

### 3. Conclusions

In this work, two new microfluidic paper-based analytical devices ( $\mu$ PADs) for the nitrite and nitrate quantification in human saliva samples, were devised. The main application envisioned for these devices was for them to facilitate the diagnosis of some diseases and health conditions, not only in healthcare facilities, but also in remote areas.

In conclusion, the developed  $\mu$ PADs for nitrite and nitrate determination have shown to be sensitive, portable devices that provide rapid measurements on-hand. Furthermore, unlike recently reported devices (Table 4) such as Chiang C. et al. (2019), Vidal E. et al. (2018) and Liu Y. et al. (2018) [33–35], this novel construction and assembly technique is very simple and user-friendly, since it doesn't require specialized technicians or complex equipment, like wax printers.

**Table 4.** Comparison of some features of this work with previous ones.

Analyte	Concentration Range ( $\mu$ M)	LOD ( $\mu$ M)	LOQ ( $\mu$ M)	Sample Matrix	Observations	Reference
$\text{NO}_2^-$	5 – 250	0.05	0.17	Saliva	Both determinations can be combined in a single device with a biparametric determination	This Work
$\text{NO}_3^-$	200 – 1200	80	270			
$\text{NO}_2^-$	3.9 – 1000	14.8	NR	Water	Wax printed $\mu$ PAD	Chiang [33]
$\text{NO}_2^-$	0.88 – 11.8	0.86	NR	Saliva	Sample Pretreated; Electrokinetic stacking combined with colorimetric reaction	Zhang [36]
$\text{NO}_2^-$	20 – 160	7.8	NR	Saliva	$\mu$ PAD fabrication by corona generator	Jiang [37]
$\text{NO}_2^-$	0.01 – 5.0	$6.2 \times 10^{-5}$	NR	Water	Wax printed $\mu$ PAD; Electrochemical detection	Liu [35]
$\text{NO}_2^-$	1 – 215	0.6	2.8	Water	Wax printed $\mu$ PAD	Vidal [34]
$\text{NO}_2^-$	5 – 500	1.3	2.2	Water	$\mu$ PAD fabrication by a craft-cutting technique	Ortiz-Gomez [38]
$\text{NO}_2^-$	156 – 1250	NR	NR	Water	$\mu$ PAD fabrication by patterning of filter paper using a permanent marker pen.	Wang [39]
$\text{NO}_2^-$	0 – 100	5.6	NR	Saliva	With sample preconcentration	Cardoso [40]
$\text{NO}_2^-$	10 – 150	1	7.8	Water	Inkjet printed $\mu$ PAD Independent devices for each analyte determination	Jayawardane [29]
$\text{NO}_3^-$	50 – 1000	19	48			

NR, Not Reported.

This type of printers is commonly used in  $\mu$ PADs but associated to a substantial investment, a costly up-keep and have been known not to be environmental-friendly. Most wax printers also need specialized programs to design the wax patterns.

The devices developed in this work are affordable, having a cost of 0.15€ and 0.20€ per nitrite and nitrate  $\mu$ PAD, respectively, and disposable by incineration, which besides being environmental-friendly, is also an advantage when handling biological samples.

These  $\mu$ PADs were optimized for determinations in human saliva samples without requiring complex pre-treatments and its stability studied under different conditions and periods of time. As future work, it would be interesting to perform field studies to further access the impact of conditions different from the ones that exist in the laboratory. Ultimately, the  $\mu$ PADs should be used for analysis in saliva samples of patients with NO<sub>x</sub>-related diseases.

### Acknowledgment

This work was supported by National Funds from FCT - Fundação para a Ciência e a Tecnologia through project UID/Multi/50016/2019.

### Appendix A – Supplementary Material

Additional supporting information was provided with graphic representation of preliminary studies, stability testing and accuracy assessment (Pearson plotting of the comparison with reference procedure). (ESM\_Ferreira\_et\_al.docx)

### References

- [1] World Health Organization, Standing up for the right to health, (2018). <https://www.who.int/news-room/feature-stories/detail/standing-up-for-the-right-to-health> (accessed February 22, 2019).
- [2] C.A. Petti, C.R. Polage, T.C. Quinn, A.R. Ronald, M.A. Sande, Laboratory Medicine in Africa: A Barrier to Effective Health Care, *Clin. Infect. Dis.* 42 (2006) 377–382. <https://doi.org/10.1086/499363>.
- [3] R. McNerney, Diagnostics for Developing Countries, *Diagnostics*. 5 (2015) 200. <https://doi.org/10.3390/DIAGNOSTICS5020200>.
- [4] X. Jiang, Z.H. Fan, Fabrication and Operation of Paper-Based Analytical Devices, *Annu. Rev. Anal.*

- Chem. 9 (2016) 203–222. <https://doi.org/10.1146/annurev-anchem-071015-041714>.
- [5] C.S. Kosack, A.-L. Page, P.R. Klatser, A guide to aid the selection of diagnostic tests, *Bull. World Health Organ.* 95 (2017) 639–645. <https://doi.org/10.2471/BLT.16.187468>.
- [6] Paper microfluidic devices : A review 2017 - Elveflow, (n.d.). <https://www.elveflow.com/microfluidic-tutorials/microfluidic-reviews-and-tutorials/paper-microfluidic-devices-a-review-2017/> (accessed December 13, 2018).
- [7] A.W. Martinez, S.T. Phillips, M.J. Butte, G.M. Whitesides, Patterned Paper as a Platform for Inexpensive, Low-Volume, Portable Bioassays, *Angew. Chemie.* 119 (2007) 1340–1342. <https://doi.org/10.1002/ange.200603817>.
- [8] M.I.G.S. Almeida, B.M. Jayawardane, S.D. Kolev, I.D. McKelvie, Developments of microfluidic paper-based analytical devices (μPADs) for water analysis: A review, *Talanta.* 177 (2018) 176–190. <https://doi.org/10.1016/J.TALANTA.2017.08.072>.
- [9] A.W. Martinez, S.T. Phillips, G.M. Whitesides, E. Carrilho, Diagnostics for the developing world: Microfluidic paper-based analytical devices, *Anal. Chem.* 82 (2010) 3–10. <https://doi.org/10.1021/ac9013989>.
- [10] N.C. Birch, D.F. Stickle, Example of use of a desktop scanner for data acquisition in a colorimetric assay, *Clin. Chim. Acta.* 333 (2003) 95–96. [https://doi.org/10.1016/S0009-8981\(03\)00168-2](https://doi.org/10.1016/S0009-8981(03)00168-2).
- [11] A.N. Ramdhan, M.I.G.S. Almeida, M.J. McCullough, S.D. Kolev, Development of a microfluidic paper-based analytical device for the determination of salivary aldehydes, *Anal. Chim. Acta.* 919 (2016) 47–54. <https://doi.org/10.1016/j.aca.2016.03.030>.
- [12] J.O. Lundberg, E. Weitzberg, J.A. Cole, N. Benjamin, Nitrate, bacteria and human health, in: *Nat. Rev. Microbiol.*, Nature Publishing Group, 2004: pp. 593–602. <https://doi.org/10.1038/nrmicro929>.
- [13] M.J. Moorcroft, J. Davis, R.G. Compton, Detection and determination of nitrate and nitrite: a review, *Talanta.* 54 (2001) 785–803. [https://doi.org/10.1016/S0039-9140\(01\)00323-X](https://doi.org/10.1016/S0039-9140(01)00323-X).
- [14] S.R. Tannenbaum, A.J. Sinskey, M. Weisman, W. Bishop, Nitrite in Human Saliva. Its Possible Relationship to Nitrosamine Formation<sup>23</sup>, *JNCI J. Natl. Cancer Inst.* 53 (1974) 75–784. <https://doi.org/10.1093/jnci/53.1.79>.
- [15] S.S. Mirvish, K.J. Reimers, B. Kutler, S.C. Chen, J. Haorah, C.R. Morris, A.C. Grandjean, E.R. Lyden, Nitrate and nitrite concentrations in human saliva for men and women at different ages and times of the day and their consistency over time., *Eur. J. Cancer Prev.* 9 (2000) 335–42. <https://doi.org/10.1097/00008469-200010000-00008>.
- [16] Atsdr, Toxicological Profile for Nitrate and Nitrite, n.d. <https://www.atsdr.cdc.gov/ToxProfiles/tp204-c3.pdf> (accessed September 25, 2018).

- [17] B.M. Jayawardane, I.D. McKelvie, S.D. Kolev, Development of a gas-diffusion microfluidic paper-based analytical device ( $\mu$ PAD) for the determination of ammonia in wastewater samples, *Anal. Chem.* 87 (2015) 4621–4626. <https://doi.org/10.1021/acs.analchem.5b00125>.
- [18] P. Kerkar, What is Blue Baby Syndrome & How is it Treated?, (2018). <https://www.epainassist.com/blood-diseases/what-is-blue-baby-syndrome-and-how-is-it-treated> (accessed May 25, 2018).
- [19] G.A. Sánchez, V.A. Miozza, A. Delgado, L. Busch, Total salivary nitrates and nitrites in oral health and periodontal disease, *Nitric Oxide.* 36 (2014) 31–35. <https://doi.org/10.1016/J.NIOX.2013.10.012>.
- [20] J.J. Doel, M.P. Hector, C. V. Amirtham, L.A. Al-Anzan, N. Benjamin, R.P. Allaker, Protective effect of salivary nitrate and microbial nitrate reductase activity against caries, *Eur. J. Oral Sci.* 112 (2004) 424–428. <https://doi.org/10.1111/j.1600-0722.2004.00153.x>.
- [21] L.F. Hofman, Human Saliva as a Diagnostic Specimen, *J. Nutr.* 131 (2001) 1621S–1625S. <https://doi.org/10.1093/jn/131.5.1621S>.
- [22] S. Chojnowska, T. Baran, I. Wilińska, P. Sienicka, I. Cabaj-Wiater, M. Knaś, Human saliva as a diagnostic material, *Adv. Med. Sci.* 63 (2018) 185–191. <https://doi.org/10.1016/J.ADVMS.2017.11.002>.
- [23] M. Tiwari, Science behind human saliva, *J. Nat. Sci. Biol. Med.* 2 (2011) 53–58. <https://doi.org/10.4103/0976-9668.82322>.
- [24] S. Chiappin, G. Antonelli, R. Gatti, E.F. De Palo, Saliva specimen: A new laboratory tool for diagnostic and basic investigation, *Clin. Chim. Acta.* 383 (2007) 30–40. <https://doi.org/10.1016/J.CCA.2007.04.011>.
- [25] E.A. Almeida, P.D.V, Saliva Composition and Functions: A Comprehensive Review, *J. Comtemporary Dent. Pract.* Vol. 9, 9 (2008) 72–80.
- [26] G. Eisenbrand, B. Spiegelhalder, R. Preussmann, Nitrate and nitrite in saliva., *Oncology.* 37 (1980) 227–31. <https://doi.org/10.1159/000225441>.
- [27] C.F.C.P. Teixeira, R.L.A. Segundo, A.O.S.S. Rangel, R.B.R. Mesquita, M.T.S.O.B. Ferreira, A.A. Bordalo, Development of a sequential injection system for the determination of nitrite and nitrate in waters with different salinity: Application to estuaries in NW Portugal, *Anal. Methods.* 1 (2009) 195–202. <https://doi.org/10.1039/b9ay00101h>.
- [28] APHA, AWWA, WEF, Standard Methods for the Examination of Water and Wastewater, 20th ed., Washington, DC, 1998.
- [29] B.M. Jayawardane, S. Wei, I.D. McKelvie, S.D. Kolev, Microfluidic Paper-Based Analytical Device for the Determination of Nitrite and Nitrate, *Anal. Chem.* 86 (2014) 7274–7279.



- <https://doi.org/10.1021/ac5013249>.
- [30] A. Wiegand, G.R. Batista, C.R.G. Torres, B. Sener, T. Attin, Artificial Saliva Formulations versus Human Saliva Pretreatment in Dental Erosion Experiments, *Caries Res.* 50 (2016) 78–86. <https://doi.org/10.1159/000443188>.
- [31] L.A. Currie, Nomenclature in evaluation of analytical methods including detection and quantification capabilities (IUPAC Recommendations 1995), *Pure Appl. Chem.* 67 (1995) 1699–1723. <https://doi.org/10.1351/pac199567101699>.
- [32] D.T. Burns, K. Danzer, A. Townshend, Use of the term “recovery” and “apparent recovery” in analytical procedures (IUPAC Recommendations 2002), *Pure Appl. Chem.* 74 (2002) 2201–2205. <https://doi.org/10.1351/pac200274112201>.
- [33] C.-K. Chiang, A. Kurniawan, C.-Y. Kao, M.-J. Wang, Single step and mask-free 3D wax printing of microfluidic paper-based analytical devices for glucose and nitrite assays, *Talanta*. 194 (2019) 837–845. <https://doi.org/10.1016/j.talanta.2018.10.104>.
- [34] E. Vidal, A.S. Lorenzetti, A.G. Lista, C.E. Domini, Micropaper-based analytical device ( $\mu$ PAD) for the simultaneous determination of nitrite and fluoride using a smartphone, *Microchem. J.* 143 (2018) 467–473. <https://doi.org/10.1016/j.microc.2018.08.042>.
- [35] Y.-C. Liu, C.-H. Hsu, B.-J. Lu, P.-Y. Lin, M.-L. Ho, Determination of nitrite ions in environment analysis with a paper-based microfluidic device, *Dalt. Trans.* 47 (2018) 14799–14807. <https://doi.org/10.1039/C8DT02960A>.
- [36] X.X. Zhang, Y.Z. Song, F. Fang, Z.Y. Wu, Sensitive paper-based analytical device for fast colorimetric detection of nitrite with smartphone, *Anal. Bioanal. Chem.* (2018) 1–5. <https://doi.org/10.1007/s00216-018-0965-2>.
- [37] Y. Jiang, Z. Hao, Q. He, H. Chen, A simple method for fabrication of microfluidic paper-based analytical devices and on-device fluid control with a portable corona generator, *RSC Adv.* 6 (2016) 2888–2894. <https://doi.org/10.1039/c5ra23470k>.
- [38] I. Ortiz-Gomez, M. Ortega-Muñoz, A. Salinas-Castillo, J.A. Álvarez-Bermejo, M. Ariza-Avidad, I. de Orbe-Payá, F. Santoyo-Gonzalez, L.F. Capitan-Vallvey, Tetrazine-based chemistry for nitrite determination in a paper microfluidic device, *Talanta*. 160 (2016) 721–728. <https://doi.org/10.1016/j.talanta.2016.08.021>.
- [39] B. Wang, Z. Lin, M. Wang, Fabrication of a paper-based microfluidic device to readily determine nitrite ion concentration by simple colorimetric assay, *J. Chem. Educ.* 92 (2015) 733–736. <https://doi.org/10.1021/ed500644m>.
- [40] T.M.G. Cardoso, P.T. Garcia, W.K.T. Coltro, Colorimetric determination of nitrite in clinical, food and environmental samples using microfluidic devices stamped in paper platforms, *Anal.*

Methods. 7 (2015) 7311–7317. <https://doi.org/10.1039/c5ay00466g>.

Journal Pre-proof

**Declaration of interests**

☒ The authors declare that they have no known competing financial interests or personal relationships that could have appeared to influence the work reported in this paper.

☐ The authors declare the following financial interests/personal relationships which may be considered as potential competing interests: